Electronic Supplementary Information for:

Surpassing the Use of Copper in the Click Functionalization of Polymeric Nanostructures: A Strain-Promoted Approach

Enrique Lallana, Eduardo Fernandez-Megia,* and Ricardo Riguera*

Departamento de Química Orgánica, Facultad de Química, and Unidad de RMN de Biomoléculas Asociada al CSIC, Universidad de Santiago de Compostela, Avda. de las Ciencias S.N. 15782 Santiago de Compostela, Spain.

Table of Contents

Manuscript reference 4b: Aktas, Y.; Yemisci, M.; Andrieux, K.; Gürsoy, R. N.; Alonso, M. J.; Fernandez-Megia, E.; Novoa-Carballal, R.; Quiñoá, E.; Riguera, R.; Sargon, M. F.; Çelik, H. H.; Demir, A. S.; Hıncal, A. A.; Dalkara, T.; Çapan, Y.; Couvreur, P. *Bioconjugate Chem.* **2005,** *16*, 1503.

Materials. Ultrapure chitosan (CS) hydrochloride salt [Protasan UP CL 113, degree of acetylation (DA) 14% by ^{1}H NMR][1] was purchased from Pronova Biomedical A.S. (Norway). Dextran from *Leuconostoc menesteroides* and mannan from *Saccharomyces cerevisiae* were purchased from Fluka. Hyaluronic acid sodium salt from rooster comb was purchased from Sigma. Heterodifunctional PEG **1** was purchased from Nektar (USA), (M_n 3837, M_w 3890, by MALDI-TOF). Anti-Bovine Serum Albumin (BSA) Rabbit IgG was purchased from Invitrogen (2.0 mg/mL). Horseradish Peroxidase (HRP) conjugated Goat Anti-Rabbit IgG (1.0 mg/mL), CL-XPosure™ film, Luminol/Enhancer Solution® and Stable Peroxide Solution® were purchased from Pierce. Albumin (BSA) Agarose beads (BSA-Agarose beads, 10.1 mg/mL in 0.5 M NaCl containing 0.02 % thimerosal) were purchased from Sigma, and were washed with and resuspended in 10 mM Phosphate Buffer Saline (PBS) pH 7.4, 150 mM NaCl before use. 2,4-dinitrophenyhydrazine, cysteine, homopropargylic alcohol, sodium ascorbate, and Cu turnings were purchased from Aldrich. $CuSO_4 \cdot 5H_2O$ was obtained from Prolabo (Spain). Sulfonated bathophenanthroline disodium salt was purchased from Alfa Aesar. $[Cu(MeCN)_4][PF_6]$ was prepared as previously reported.[2] All other reagents used were of analytical grade.

General Methods. CH_2Cl_2, $CHCl_3$, Et_3N, MeCN, *i*-PrOH, DIPEA, and pyridine were distilled from CaH_2. Toluene was distilled from Na/benzophenone, and MeOH from Mg. DMF was dried over 4Å ms. Thin-layer chromatography (TLC) was done on silica 60/F-254 aluminum-backed plates. Column chromatography was performed with 70-230 and 230-400 mesh silica gel. Ultrafiltration was carried out with Amicon® stirred cells [YM30 (MWCO 30000 Da) and YM3 (MWCO 3000 Da) membranes]. Centrifugal ultrafiltration was carried out with Amicon® Ultra-4 centrifugal filters (50K NMWL).

MALDI-TOF MS. MALDI-TOF experiments were carried out on a Bruker Autoflex operating in reflected mode. 2-(4-Hydroxyphenylazo)benzoic acid (HABA) was used as matrix, and NaCl or KCl as cationizing agent. Samples were dissolved in MeOH-H_2O (1:1) at a concentration $5 \cdot 10^{-4}$ M. HABA was dissolved in dioxane at a concentration 0.05 M. Sample (20 μL) and matrix (80 μL) solutions were mixed, and then 80 μL of 0.02 M NaCl or KCl was added. Finally, 1 μL of the resulting mixture was placed on the MALDI plate.

SEC-MALLS. The M_w of the commercial polysaccharides CS ($8.0 \cdot 10^4$ g/mol), mannan ($3.6 \cdot 10^4$ g/mol), dextran ($6.6 \cdot 10^4$ g/mol), and hyaluronic acid ($8.2 \cdot 10^5$ g/mol) were determined by size exclusion chromatography-multiangle laser-light scattering (SEC-MALLS). An Iso Pump G1310A (Hewlett Packard) was connected to a PSS Novema GPC column (10 μm, 30 Å, 8×300 mm, NOA0830103E1), and a PSS Novema GPC column (10 μm, 3000 Å, 8×300 mm, NOA0830103E3). A PSS SLD7000 MALLS detector (Brookhaven Instruments Corporation) operating at 660 nm, and a G1362A refractive index detector (Agilent) were connected on line. Polymer concentrations around 3.0 mg/mL for CS (dissolved in 0.15 M NH_4OAc, 0.2 M AcOH buffer, pH 4.5), and 2.5 mg/mL for the other polymers (mannan dissolved in 0.1 M $NaNO_3$ containing 0.5 mg/mL NaN_3, dextran dissolved in H_2O, and hyaluronic acid in 2 mM PBS pH 7.3 containing 145 mM NaCl) were typically employed. Solutions were filtered through 0.2 μm pore size membranes before injection. Refractive index increment dn/dc was set at 0.188 for CS,[3] 0.162 for mannan,[4] 0.147 for dextran,[5] and 0.167 for hyaluronic acid.[6]

NMR Spectroscopy. NMR spectra were recorded at 250, 400, and 750 MHz spectrometers in D_2O, 2% DCl in D_2O, $CDCl_3$, or *d*-DMSO. Chemical shifts are reported in ppm (δ units) downfield from residual solvent peak (*d*-DMSO), or internal tetramethylsilane ($CDCl_3$) and 3-(trimethylsilyl)-propionic acid-d_4 (D_2O).

The degree of substitution (DS) of the graft copolymers CS-*g*-PEG-N_3 (**5**) was determined by integration of the appropriate signals in the ^{1}H NMR spectra (2% DCl in D_2O, rt) after partially hydrolysing the sample by heating in 2% DCl at 70 ºC for 8 h. Intervals of integration: 2.20-2.05 ppm (CS acetyl groups), 4.30-3.05 ppm (H2-H6 of CS, CH_2 of PEG, and protons of the linkers and bioactive molecules/tags falling in this δ range).

The progress of the click functionalization of **5** and the characterization of the resulting clicked CS-*g*-PEG polymers were better performed by presat ^{1}H NMR experiments at the water solvent peak. Thus, under these experimental conditions, not only the water peak was completely saturated, but the intensity of all CS resonances was mostly reduced, leading to cleaner spectra with enhanced resolution for the resonances of PEG. Figure S1 shows the ^{1}H NMR spectra of **5** (DS 2.8) under standard and presat conditions (D_2O, 750 MHz). Clearly, the filtering of the resonances of CS and linkers close to the CS backbone (***f***,***g***,***h***) in the presat experiment, allows an easier monitoring of the progress of the click functionalizations by disappearance of the methylene protons ***b*** (1.8 ppm) and ***c*** (3.3 ppm), β and γ to the azide group. A possible explanation accounting for this effect is saturation transfer from water, firstly to labile OH and NH protons of CS, and ultimately to CS backbone protons. Alternatively, saturation transfer could start at the CS anomeric protons, as they are also certainly affected by the saturation pulse.

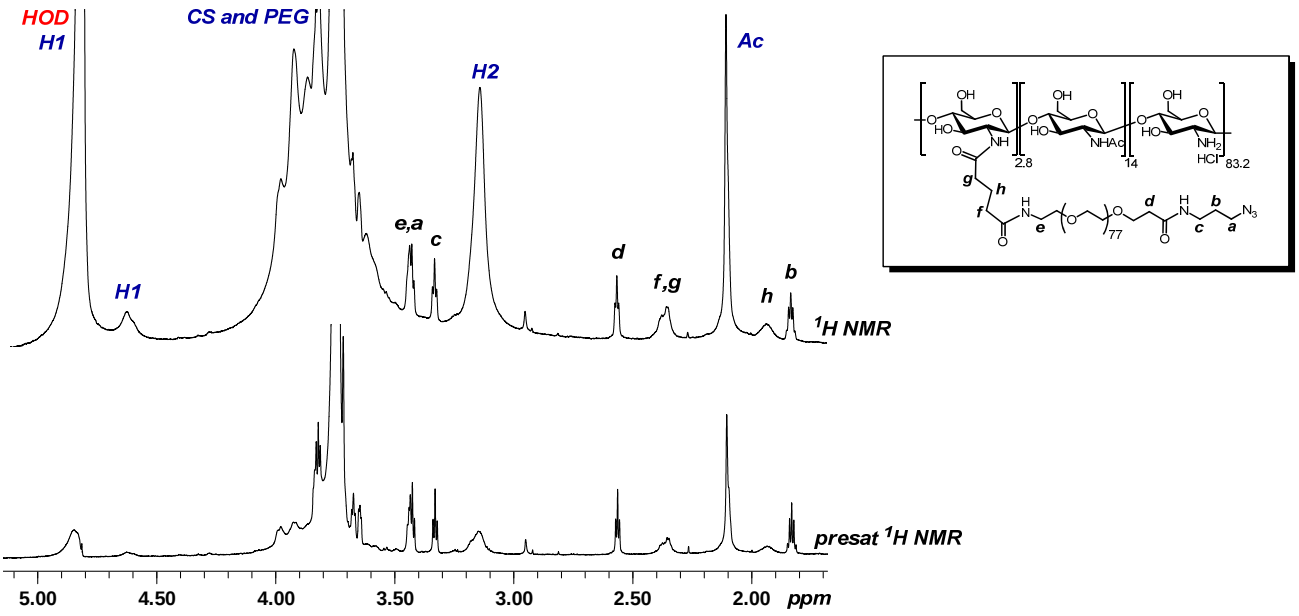

Figure S1. ^{1}H NMR spectra (D_2O, 750 MHz, 6 mg/mL, 25 ºC) of **5** (DS 2.8) under standard (acquisition time 1 s, delay time 9 s) and presat conditions (acquisition time 1 s, delay time 7 s, saturation time 2 s, saturation power 2 dB).

Overview of Depolymerization of Polysaccharides in the Presence of Transition Metal Ions and/or Ascorbate. Various redox strategies have been mentioned in the manuscript to collectively produce $^{\bullet}$OH as the final reactive oxygen species (ROS) able to degrade polysaccharides and other biomacromolecules. Thus, from the reduced form of a transition metal, Cu(I) in our case, and H_2O_2, $^{\bullet}$OH can be generated through a Fenton reaction, as shown in eq. S1.

$$Cu(I) + H_2O_2 \rightarrow Cu(II) + {}^{\bullet}OH + OH^- \quad (S1)$$

The required H_2O_2 in eq. S1 can be produced *in situ* through two possible mechanisms:

i) Cu(II)-catalyzed reduction of O_2 by ascorbate (AH_2) (eq. S2).

$$AH_2 + O_2 \rightarrow A + H_2O_2 \quad (S2)$$

ii) In the absence of other reducing agents, H_2O_2 can be obtained through a two step process involving the superoxide anion radical ($O_2^{\bullet-}$) as intermediate (eq. S3-S4).

$$Cu(I) + O_2 \rightarrow O_2^{\bullet-} + Cu(II) \quad (S3)$$

$$Cu(I) + O_2^{\bullet-} + 2H^+ \rightarrow Cu(II) + H_2O_2 \quad (S4)$$

Under this set of conditions several polysaccharides have been reported to depolymerize. Thus, for example, the simple addition of ascorbate is reported to produce the depolymerization of polysaccharides, such as xyloglucan, carboxymethylcellulose, pectin, dextran, alginate, and methylcellulose, thanks to the presence of endogeneous trace amounts of transition metal ions within these polysaccharides.[7] Similarly, several plant cell wall polysaccharides (xylan, galacturonan, arabinogalactan, and cellulose) suffer depolymerization when incubated with H_2O_2,[8] probably again as a result of the presence of Cu(II) within the polymers, and the possibility of its reduction to Cu(I) by H_2O_2.[9,10] Also, the addition of Fe(II) salts to hyaluronic acid (HA) in the presence of O_2 has allowed the production of low MW HA, again through a process mediated by $^{\bullet}OH$.[11] Similar behavior has been observed for chondroitin sulphate.[12]

Indeed, the most efficient depolymerization conditions have been claimed by the simultaneous addition of ascorbate and a transition metal (Cu being more effective than Fe). Under these conditions, a higher concentration of the active $^{\bullet}OH$ results, and drastic depolymerizations have been reported for pullulan, carboxymethylcellulose, HA, welan, glucan, and β-CD.[13,14,15,16]

Overview of the Depolymerization of Chitosan with $^{\bullet}OH$. Indeed, several reports on the depolymerization of CS with $^{\bullet}OH$ [obtained by the addition of: Cu(II)-ascorbate,[17] Cu(II)-H_2O_2,[18] Fe(III)-H_2O_2,[19] H_2O_2,[20,21] or ascorbate[22]] have been reported in the literature. The effectiveness of this depolymerization process is illustrated by the fact that some of these procedures actually pursued the controlled depolymerization of CS.[18,20] Another example takes advantage of the high tendency of CS to react with ROS to employ it as scavenger offering protection against DNA damage.[23]

Some of these reports have studied in detail the mechanism of degradation of CS.[17,20,24] It has been revealed the importance of the coordination of Cu ions to the amino groups of CS. Thus, not only the *N*-acetyl groups of CS have shown to slow down the rearrangement of radicals during β-cleavage, but chitin itself proved to be stable under these depolymerization conditions. As a result, it has been

proposed the amino groups of CS to facilitate the depolymerization by favoring the generation of $^{\bullet}OH$ close to the Cu-NH_2 binding site, and these radicals to cut off chitosan at the near position through the formation of carbon-centered radicals at the glycosidic linkage. This explains the faster degradation of CS with lower degrees of acetylation.

The close proximity of the newly generated radicals to the CS backbone explains the low efficiency of classical radical scavengers, such as mannitol, formate, benzoate, thiourea, DMSO, or DMF, in preventing CS depolymerization. Thus, although these scavengers are able to drastically reduce the depolymerization of various polysaccharides,[7] in the case of CS solutions they cannot avoid the reduction of the intrinsic viscosity to values around 50% of the initial value.[17,18,20]

Once the depolymerization has started, CS chains of lower MW and increased solubility appeared. Under these conditions, some of the bound metal ions might be released from the smaller CS chains, leading to $^{\bullet}OH$ in solution that are able to attack soluble chitosan molecules more easily, especially on the more mobile sections close to the chain ends. At this stage of the degradation, the production of glucosamine and chito-oligosaccharides increases significantly, and the process becomes a combination of random and chain-end scissions.[20]

Quantification of the Polysaccharide Depolymerizations under CuAAC Conditions. In order to study the depolymerization of polysaccharides under CuAAC we selected the least depolymerizing conditions found for CS-*g*-PEG. Briefly, solutions of CS (M_w $8.0\cdot10^4$ g/mol) and other representative polysaccharides [mannan (M_w $3.6\cdot10^4$ g/mol), dextran (M_w $6.6\cdot10^4$ g/mol), and hyaluronic acid (M_w $8.2\cdot10^5$ g/mol)] were prepared (5.0 mg/mL) in: CS (0.34 M NH_4OAc, 0.01 M AcOH buffer, pH 6.5), mannan (0.1 M $NaNO_3$ containing 0.5 mg/mL NaN_3), dextran (H_2O), and hyaluronic acid (2 mM PBS pH 7.3 containing 145 mM NaCl). $CuSO_4\cdot5H_2O$ (0.4 mg/mL) and Cu turnings were added and then pH was readjusted to 6.5-7.0 with aq NaOH. Reactions were allowed to stir at rt overnight. The pH was then lowered to 3.0 with aq HCl and Dowex M4195 was added with the aim of removing Cu ions.

In the case of mannan, dextran, and hyaluronic acid, the mixtures were orbitally shaken overnight. A slight precipitation observed during the Cu(II)/Cu treatment was completely removed during the first hours of shaking. Then, the resin was removed by filtration and the pH was adjusted to 7.0 (mannan and dextran) or 7.3 (hyaluronic acid) with aq NaOH prior SEC-MALLS analysis.

In the case of CS, the precipitation was more noticeable during the Cu(II)/Cu treatment, and dilution of the sample at pH 3.0 with 10^{-3} M HCl was necessary before Dowex M4195 being added. After 24 h of orbital shaking, the resin was removed by filtration and the mixture was concentrated by ultrafiltration (Amicon® YM3; 0.15 M NH_4OAc, 0.2 M AcOH, pH 4.5) before SEC-MALLS analysis. Since ultrafiltration discards polymers with the lowest range of molecular weights, it is believed the depolymerisation of CS under Cu catalyzed click conditions to be more severe than determined by SEC-MALLS.

SEC-MALLS analysis of the four samples were performed as indicated above, revealing the following M_w values: CS ($4.2 \cdot 10^3$ g/mol), mannan ($3.5 \cdot 10^4$ g/mol), dextran ($4.1 \cdot 10^4$ g/mol), and hyaluronic acid ($9.8 \cdot 10^3$ g/mol). In the absence of Cu, the integrity of CS, mannan, dextran, and hyaluronic acid during the Dowex M4195 acidic treatment was confirmed by SEC-MALLS.

Detection of $^{\bullet}OH$ Produced under CuAAC Conditions by DMSO Trapping and HPLC. Detection of $^{\bullet}OH$ produced in the reaction medium under CuAAC conditions was performed by HPLC-UV following a slightly modified procedure reported by Jiang and co-workers.[25] This procedure is based on the trapping of $^{\bullet}OH$ by DMSO leading to formaldehyde, that after reaction with 2,4-dinitrophenylhydrazine (DNPH) gives the corresponding 2,4-dinitrophenylhydrazone (DNPHo). Analysis of the reaction mixture by HPLC-UV allows the indirect detention of $^{\bullet}OH$.

For the HPLC-UV analyses, a Waters 515 HPLC pump, an analytical Waters Sperisorb® ODS2-C18 column (250 × 4.6 mm, particle size 5 μm), and a Waters 2487 detector operating at 355 nm were connected on line. An isocratic elution was performed using a mixture of MeOH/H_2O (60:40, v/v) as

mobile phase, at a flow rate of 1.5 mL/min. Under these experimental conditions, DNPH and DNPHo showed retention times around 5.0 and 11.5 min, respectively.

Experimental Procedure. DMSO (0.18 mL) was added to solutions of $CuSO_4 \cdot 5H_2O$ (1.8 mL, 0.44 mg/mL in 5% *t*-BuOH/H_2O) containing sodium ascorbate (1.58 mg/mL) or Cu turnings. Then, the pH was adjusted to 7.0 with aq. NaOH, and solutions were diluted with 5% *t*-BuOH/H_2O up to a total volume of 2.18 mL. Reactions were allowed to stir overnight at rt. Afterwards, 0.3 mL of each mixture were added to solutions of EDTA disodium salt (0.7 mL, 2.68 mg/mL) in H_3PO_4/NaH_2PO_4 buffer (30 mM, pH 4.0). The resulting mixtures (1.0 mL) were added to ready prepared solutions of DNPH (1.0 mL, 0.023 mg/mL in H_2O) and allowed to stir at rt for 4 h, before being analyzed by HPLC-UV (Figure S2).

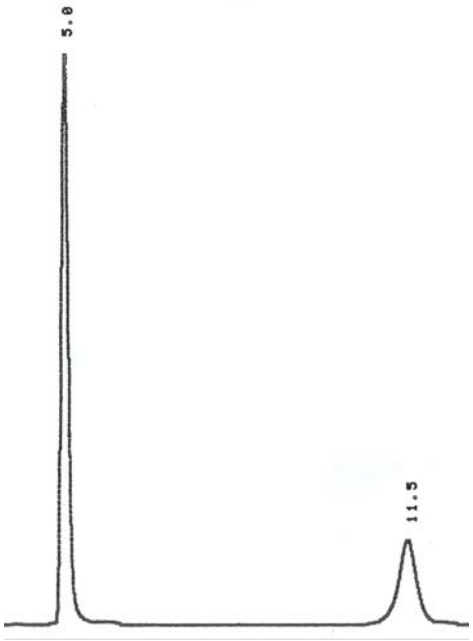

Figure S2. HPLC-UV chromatogram for the detection of $^{\bullet}OH$ produced under CuAAC conditions by DMSO/DNPH trapping. Peaks at 5.0 and 11.5 min correspond to DNPH and DNPHo, respectively.

Flame Atomic Absorption Spectrometry (FAAS). Residual Cu content in the clicked graft copolymer **6** was determined by FAAS in a Perking Elmer Atomic Absorption Spectrometer 3110, following polymer degradation. Briefly, PEG-grafted CS **6** was dissolved in 2% aq AcOH at a concentration of 3.0 mg/mL. Then, $NaNO_2$ was added to a final concentration of 0.1 M and the resulting solution was heated at 50 ºC overnight. After cooling down to rt, the atomic absorption was measured at the resonance line of 324.8 nm, under manufacturer recommended conditions. The concentration of Cu in **6** was determined by comparison with a calibration curve obtained from standards of known Cu concentration after subtraction of the Cu content in the $NaNO_2$/2% acetic acid solution. Cu content in starting CS (15.0 mg/mL in 2% aq AcOH) was also measured for comparison purposes following a similar procedure to the one described above.

Table S1. Concentration of Cu present in starting CS and clicked CS-*g*-PEG **6** determined by FAAS.

Sample	**Cu(I) source**	**Added Cu(II) (mol% per N_3)**	**Work-up**	**Found Cu (ppm)**
6 (DS 2.8)	Cu(II)/Cu	6000	Amberlite IR-120, pH 3, 24 h	696±33
6 (DS 2.8)	Cu(II)/Ascorbate	6000	Dowex M-4195, pH 3, 24 h	212±11
CS	-	-	-	nd

Figure S3. Picture of starting CS-*g*-PEG-N_3 **5** (left) and clicked CS-*g*-PEG **6** after CuAAC (right).

Dynamic Light Scattering (DLS). DLS measurements were performed on a Malvern Nano ZS (Malvern Instruments, U.K.), operating at 633 nm with a 173º scattering angle. Samples were measured at a final concentration of 0.1 mg/mL diluted with MilliQ water.

Transmission Electron Microscopy (TEM). TEM measurements were performed on a Philips CM-12 electron microscope. A drop of a solution of NP **19** in H_2O (0.1 mg/mL) was settled on a Formvar precoated copper grid, and allowed to dry at rt for 24 h. Negative staining was performed by using a droplet of 1% phosfotungstic acid, which was allowed to contact the sample for 1 min, before being washed with distilled water. An average diameter of 47±11 nm was determined by measuring the size of about 50 nanoparticles using ImageJ software.

Atomic Force Microscopy (AFM). Samples for AFM imaging were prepared by depositing the aqueous solution of NP **19** onto Si wafers. The AFM imaging was performed in air using a Multimode NanoScope V system (Veeco, Santa Barbara, CA) operated in tapping mode. Tip Characteristics: 1-10 OHm-cm Phosphorus (n) dopped Si. Cantilever T: 3.5 - 4.5 μm. Frecuency: 257-342 KHz. Tip ROC < 10 nm. Tip ROC MAx: 12.5 nm. An average diameter of 54±15 nm was determined by measuring the size of about 50 nanoparticles using ImageJ software.

Synthesis and Characterization of New Compounds:

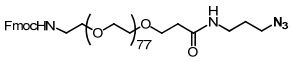

N_3-PEG-NHFmoc (2). 1-Azido-3-aminopropane[26] (13 mg, 0.126 mmol, 500 mol%) was added to a solution of heterodifunctional PEG **1** (100 mg, 0.025 mmol; M_n 3837, M_w 3890, by MALDI-TOF) in CH_2Cl_2 (2.5 mL). The resulting solution was stirred at rt for 24 h under Ar. After evaporation of the solvent, the crude product was dissolved in CH_2Cl_2 (1 mL), was precipitated by the addition of Et_2O (~200 mL) and filtered to give **2** (97 mg, 97%) as a white powder: ^{1}H NMR (400 MHz, $CDCl_3$, 333 K) δ: 7.74 (d, *J*=7.7 Hz, 2H), 7.59 (d, *J*=7.4 Hz, 2H), 7.37 (dt, *J*=1.0 Hz, *J*=7.4 Hz, 2H), 7.29 (dt, *J*=1.0 Hz, *J*=7.4 Hz, 2H), 6.50 (br s, 1H), 5.24 (br s, 1H), 4.41 (d, *J*=6.8 Hz, 2H), 4.21 (t, *J*=6.8 Hz, 1H), 3.82-3.77 (m, 2H), 3.75-3.50 (m, ~320H), 3.46-3.43 (m, 2H), 3.39-3.28 (m, 6H), 2.44 (t, *J*=5.7 Hz, 2H), 1.79 (quint, *J*=6.8 Hz, 2H); MALDI-TOF MS *m*/*z*: M_n 3848, M_w 3862, M_p 3826 $[M+H]^+$. Calcd.: M_n 3837, M_p 3827 $[M+H]^+$.

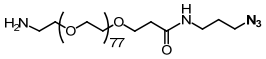

N_3-PEG-NH_2 (3). Octane-1-thiol (42 µL, 0.243 mmol, 1000 mol%) and DBU (4 µL, 0.024 mmol, 100 mol%) were sequentially added to a solution of N_3-PEG-NHFmoc (**2**) (97 mg, 0.024 mmol) in CH_2Cl_2 (2.4 mL). The resulting solution was stirred at rt for 24 h under Ar. Then, the solvent was evaporated, and the resulting crude product was dissolved in CH_2Cl_2 (1 mL), precipitated by the addition of Et_2O/*i*-PrOH (9:1, ~200 mL), and filtered to give **3** (85 mg, 93%) as a white powder: ^{1}H NMR (400 MHz, $CDCl_3$, 330K) δ: 6.52 (br s, 1H), 3.83-3.78 (m, 2H), 3.77-3.54 (m, ~320H), 3.48-3.41 (m, 2H), 3.36-3.30 (m, 4H), 3.00 (t, *J*=5.0 Hz, 2H), 2.44 (t, *J*=5.7 Hz, 2H), 1.79 (quint, *J*=6.8 Hz, 2H); ^{13}C NMR (100 MHz, $CDCl_3$, 300K) δ: 171.7, 70.4, 67.1, 49.0, 40.9, 36.7, 36.5, 28.6; MALDI-TOF MS *m*/*z*: M_n 3654, M_w 3688, M_p 3653 $[M+H]^+$. Calcd.: M_n 3615, M_p 3605 $[M+H]^+$.

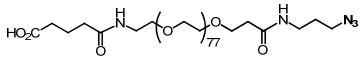

N_3-PEG-CO_2H (4). Glutaric anhydride (13 mg, 0.115 mmol, 500 mol%) was added to a solution of N_3-PEG-NH_2 (**3**) (85 mg, 0.023 mmol) in pyridine (2.3 mL). After 24 h of stirring at rt under Ar, the solvent was evaporated and the resulting crude product was dissolved in MeOH (5 mL). Amberlite IR-120 was added to remove traces of pyridine, and after 1 h of orbital shaking, the resin was filtered off. The filtrate was concentrated, and then dissolved in CH_2Cl_2 (1 mL), precipitated by the addition of Et_2O (~200 mL), and filtered to give **4** (84 mg, 96%) as a white powder: ^{1}H NMR (400 MHz, $CDCl_3$, 330 K) δ: 6.52 (br s, 1H), 6.23 (br s, 1H), 3.83-3.78 (m, 2H), 3.77-3.54 (m, ~320H), 3.48-3.41(m, 4H), 3.36-3.29 (m, 4H), 2.45 (t, *J*=5.7 Hz, 2H), 2.39 (t, *J*=6.8 Hz, 2H), 1.97 (quint, *J*=7.0 Hz, 2H), 1.80 (quint, *J*=6.7 Hz, 2H); ^{1}H NMR (400 MHz, D_2O, 300 K) δ: 3.94-3.89 (m, 2H), 3.85-3.62 (m, ~320H), 3.56-3.53 (m, 2H), 3.42-3.39 (m, 4H), 3.32 (t, *J*=6.7 Hz, 2H), 2.54 (t, *J*=6.0 Hz, 2H), 2.43 (t, *J*= 7.4 Hz, 2H), 2.34 (t, *J*=7.5 Hz, 2H), 1.92 (quint, *J*=7.5 Hz, 2H), 1.82 (quint, *J*=6.7 Hz, 2H); ^{13}C NMR (100 MHz, $CDCl_3$, 300K) δ: 174.5, 172.5, 171.8, 70.4, 70.2, 70.1, 70.0, 69.7, 67.1, 49.1, 39.1, 36.8, 36.6, 35.0, 32.7, 26.7, 20.8; MALDI-TOF MS *m*/*z*: M_n 3723, M_w 3752, M_p 3723 $[M+H]^+$. Calcd.: M_n 3729, M_p 3719 $[M+H]^+$.

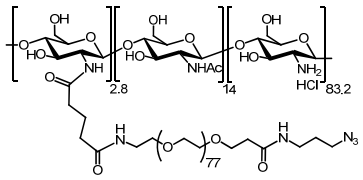

CS-*g*-PEG-N_3 (5) (DS 2.8). CS·HCl (90 mg, 0.453 mmol, DA 14%, M_w $8.0\cdot10^4$ g/mol), N_3-PEG-CO_2H (**4**) (53 mg, 14.1 μmol), and HOBt (9.2 mg, 68.1 μmol) were dissolved in H_2O (12.9 mL). Then, EDC·HCl (65.4 mg, 0.341 mmol) was added in four equal portions every 30 min. The resulting solution was stirred overnight, and then was ultrafiltered (Amicon® YM30, 10^{-3} M HCl) and lyophilized to afford **5** (128 mg, DS 2.8 by ^{1}H NMR, 90% yield of grafting , 90% mass recovery) as a white foam: ^{1}H

NMR (400 MHz, 2% DCl in D_2O, 300K) δ: 5.00-4.51 (m), 4.30-3.34 (m, 1416H), 3.30-3.05 (m, 87H), 2.52 (t, *J*=5.9 Hz), 2.38-2.27 (m), 2.20-2.05 (m, 41H), 1.99-1.88 (m), 1.83 (quint, *J*=6.7 Hz).

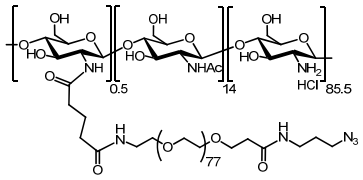

CS-*g*-PEG-N_3 (5) (DS 0.5). From CS·HCl (132 mg, 0.665 mmol), N_3-PEG-CO_2H (**4**) (15 mg, 4.01 μmol), HOBt (2.7 mg, 20.0 μmol), and EDC·HCl (37 mg, 0.192 mmol) dissolved in H_2O (18.9 mL), and following the same experimental procedure as above, CS-*g*-PEG-N_3 (**5**) was obtained as a white foam (142 mg, DS 0.5 by ^{1}H NMR, 83% yield of grafting, 97% mass recovery): ^{1}H NMR (400 MHz, 2% DCl in D_2O, 300K) δ: 5.00-4.51 (m), 4.30-3.34 (m, 689H), 3.30-3.05 (m, 86H), 2.52 (t, *J*=5.9 Hz), 2.38-2.27 (m), 2.20-2.05 (m, 41H), 1.99-1.88 (m), 1.83 (quint, *J*=6.7 Hz).

General Experimental Procedure for the CuAAC Functionalization of CS-*g*-PEG-N_3 (5). CS-*g*-PEG-N_3 (**5**) (DS 2.8, 25 mg, 0.083 mmol), homopropargylic alcohol (3.5 μL, 46.4 mmol, 2000 mol% per N_3), and $CuSO_4·5H_2O$ (800-6000 mol% per N_3) were dissolved in 5% *t*-BuOH/H_2O (3.5 mL). Then, sodium ascorbate (5000-30000 mol% per N_3) or Cu turnings were added. Alternatively, $[Cu(MeCN)_4][PF_6]$ was used as source of Cu(I) in the presence of sulfonated bathophenanthroline disodium salt (300 mol% per Cu). Then, the pH of the reaction was adjusted to 4.5-7.1 (aq NaOH), and 5% *t*-BuOH/H_2O was added up to a final volume of 4.2 mL. The resulting solutions were stirred for 16-72 h at rt. Then, the pH was lowered to 3.0 (aq HCl), and Dowex M4195 was added with the aim of removing Cu ions. After 24 h of orbital shaking, resin was removed by filtration, and the filtrate was ultrafiltered (Amicon® YM3, H_2O) and lyophilized.

When reactions were carried out in the absence of O_2, solutions were deoxygenated by bubbling N_2 for 20 min. When cysteine was used as radical scavenger (500 mol% per Cu), ascorbate was added as the last reagent.

Quantitative conversions were typically obtained with Cu(II)/ascorbate, and in the range 70-90% with Cu(II)/Cu as determined by ^{1}H NMR. The use of [Cu(MeCN)$_4$][PF$_6$]/sulfonated bathophenanthroline system hampered the CuAAC to proceed most probably due to ionic reticulation of the cationic CS-*g*-PEG-N_3 by the anionic sulfonated bathophenanthroline leading to polymer precipitation. In addition, no beneficial effect was observed by deoxygenation or the use of cysteine as radical scavenger.

According to SEC analysis, although both Cu(II)/ascorbate and Cu(II)/Cu systems led to various populations of depolymerized CS-*g*-PEG, this effect was stronger in the presence of ascorbate (Figure S4), in agreement with previous reports (*vide supra*).[13-16]

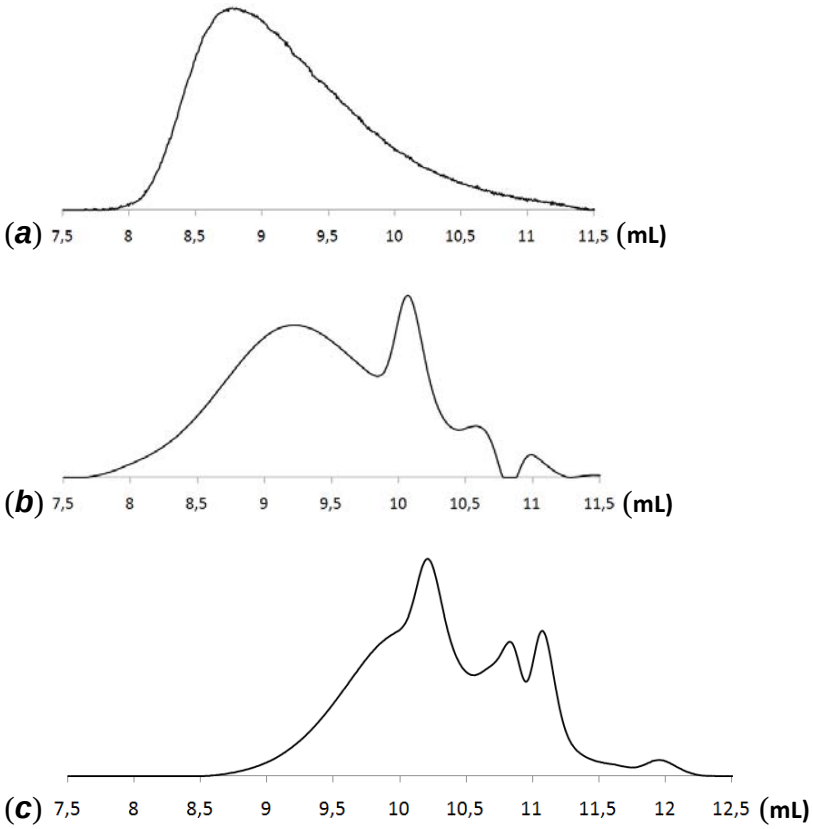

Figure S4. SEC traces (RI) for starting CS-*g*-PEG-N_3 **5** (***a***) and clicked CS-*g*-PEG **6** obtained by CuAAC under Cu(II)/Cu (***b***) and Cu(II)/ascorbate (***c***) systems (0.15 M NH_4OAc, 0.2 M AcOH, pH 4.5).

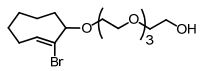

Alcohol 8. Tetraethyleneglycol (2.9 mL, 16.80 mmol, 3000 mol%) and $AgClO_4$ (348 mg, 1.69 mmol, 300 mol%) dissolved in toluene (0.7 mL) were added to a solution of **7**[27] (150 mg, 0.56 mmol) in a mixture of toluene (0.3 mL) and pyridine (0.4 mL). The reaction was refluxed in the dark for 4 h and the solvent was evaporated. Then, brine (15 mL) was added, the insoluble silver salts were removed by filtration, and the aqueous phase was extracted with Et_2O (7x30 mL). The combined organic layer was washed with brine (10 mL) and H_2O (10 mL), dried (Na_2SO_4), and concentrated to give **8** (182 mg, 85%) as a colorless oil: ^{1}H NMR (250 MHz, $CDCl_3$, 300 K) δ: 6.16 (dd, *J*=4.1 Hz, *J*=11.7 Hz, 1H), 3.90 (dd, *J*=5.1 Hz, *J*=10.1 Hz, 1H), 3.77-3.40 (m, 16H), 2.80 (br s, 1H), 2.71 (dq, *J*=5.5 Hz, *J*=11.8 Hz, 1H), 2.32-2.20 (m, 1H), 2.07-1.77 (m, 4H), 1.76-1.59 (m, 1H), 1.48 (dq, *J*=4.9 Hz, *J*=12.6 Hz, 1H), 1.34-1.17 (m, 1H), 0.81-0.69 (m, 1H); ^{13}C NMR (62 MHz, $CDCl_3$, 300K) δ: 132.9, 131.5, 85.2, 72.6, 70.51, 70.47, 70.40, 70.3, 70.2, 67.8, 61.6, 39.4, 36.4, 33.1, 27.9, 26.3; HRESIMS *m*/*z*: $[M+H]^+$. Calcd. for $C_{16}H_{29}O_5Br$, 381.1277; Found 381.1277.

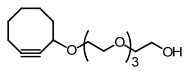

PEGO-OH (9). KO*t*Bu (103 mg, 0.915 mmol, 250 mol%) was added to a solution of **8** (110 mg, 0.366 mmol) in a mixture *i*-PrOH (2.5 mL)/pyridine (0.4 mL). After 60 h of stirring at rt, the reaction was neutralized with 5% HCl and partitioned between CH_2Cl_2 (25 mL) and H_2O (15 mL). Then, the aqueous layer was extracted with CH_2Cl_2 (7x25 mL), dried (Na_2SO_4), and concentrated under vacuum to give a crude product that was purified by column chromatography (gradient from EtOAc to EtOAc/MeOH 5%) to give **9** (90 mg, 82%) as a colorless oil: ^{1}H NMR (250 MHz, $CDCl_3$, 300 K) δ: 4.20-4.11 (m, 1H), 3.79-3.35 (m, 16H), 2.90 (br s, 1H), 1.90-1.23 (m, 10H); ^{13}C NMR (62 MHz, $CDCl_3$, 300K) δ: 100.0, 92.7, 72.7, 72.5, 70.54, 70.47, 70.45, 70.32, 70.26, 68.4, 61.7, 42.2, 34.2, 29.6, 26.3, 20.6; HRESIMS *m*/*z*: $[M+H]^+$. Calcd. for $C_{16}H_{29}O_5$, 301.2015; Found 301.2021.

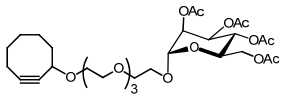

PEGO-Man-OAc (10). A solution of $BF_3{\cdot}Et_2O$ (3 µL) in CH_2Cl_2 (0.2 mL) was added dropwise to a mixture of **9** (92 mg, 0.306 mmol), tetra-*O*-acetyl-α-D-mannopyranosyl-trichloroacetimidate[28] (195 mg, 0.612 mmol, 250 mol%), and 4Å molecular sieves in CH_2Cl_2 (1.9 mL) at 0 ºC. The reaction was stirred for 12 h at 0 ºC and then allowed to gradually reach rt while being stirred for additional 12 h. After addition of a drop of Et_3N, the reaction was filtered (Celite®) and concentrated to give a crude product that was purified by column chromatography (neutral alumine deactivated with 4.8% of H_2O, EtOAc/hexane, 4/6) to give **10** (145 mg, 75%) as a colorless syrup: ^{1}H NMR (250 MHz, $CDCl_3$, 300K δ: 5.39-5.22 (m, 3H), 4.87 (d, *J*=1.4 Hz, 1H), 4.29 (dd, *J*=5.0 Hz, *J*=12.3 Hz, 1H), 4.25-4.17 (m, 1H), 4.14-4.00 (m, 2H), 3.86-3.43 (m, 16H), 2.32-1.32 (m, 22H); ^{13}C NMR (62 MHz, $CDCl_3$, 300K) δ: 170.6, 169.9, 169.8, 169.7, 100.0, 97.6, 92.7, 72.6, 70.6, 70.5, 70.4, 70.3, 69.9, 69.5, 69.0, 68.3, 67.3, 66.0, 62.3, 42.2, 34.2, 29.6, 26.3, 20.8, 20.7, 20.64, 20.61; HRESIMS *m*/*z*: $[M+Na]^+$. Calcd. for $C_{30}H_{46}O_{16}Na$, 653.2785; Found 653.2790.

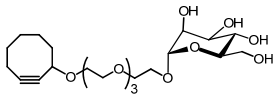

PEGO-Man (11). 1 M NaOMe in MeOH was added dropwise to a solution of **10** (45 mg, 0.071 mmol) in dry MeOH (1.4 mL) till pH 10 was reached. Then, the reaction mixture was stirred at rt for 12 h. After neutralization with Amberlite IR-120, the resin was filtered off, and the filtrate concentrated to give pure **11** (37 mg, 100%) as a colorless syrup: ^{1}H NMR (250 MHz, $CDCl_3$, 300 K) δ: 4.87 (s, 1H), 4.28-4.18 (m, 1H), 4.05-3.39 (m, 22H), 2.33-1.26 (m, 10H); ^{13}C NMR (62 MHz, $CDCl_3$, 300K) δ: 100.1, 100.0, 92.6, 72.6, 72.2, 71.3, 70.6, 70.3, 70.2, 70.0, 68.3, 66.5, 66.1, 60.7, 42.1, 34.2, 29.6, 26.3, 20.6; HRESIMS *m*/*z*: $[M+Na]^+$. Calcd. for $C_{22}H_{38}O_{10}Na$, 485.2363; Found 485.2355.

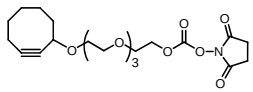

PEGO-NHS (12). *N*,*N*'-Disuccinimidyl carbonate (DSC, 255 mg, 0.999 mmol, 300 mol%) was added to a solution of **9** (100 mg, 0.333 mmol) and Et_3N (0.139 mL, 0.999 mmol, 300 mol%) in MeCN (1.3 mL). After 16 h of stirring at rt, the solvent was evaporated and reaction was partitioned between CH_2Cl_2 (30 mL) and H_2O (15mL). The aqueous layer was extracted with CH_2Cl_2 (2x30 mL), and the combined organic layer was washed with 5% $NaHCO_3$ (2x15 mL), dried (Na_2SO_4), and concentrated to give a crude that was purified by column chromatography (gradient from EtOAc/hexane 3/7 to EtOAc/hexane 1/1) to give **12** (142 mg, 97%) as a colorless syrup: ^{1}H NMR (250 MHz, $CDCl_3$, 300 K) δ: 4.49-4.43 (m, 1H), 4.27-4.18 (m, 1H), 3.82-3.77 (m, 1H), 3.76-3.46 (m, 14H), 2.84 (s, 4H), 2.33-1.35 (m, 10H); ^{13}C NMR (62 MHz, $CDCl_3$, 300K) δ: 168.5, 151.5, 99.8, 92.7, 72.6, 70.7, 70.52, 70.47, 70.40, 70.3, 70.1, 68.4, 68.2, 42.1, 34.2, 29.6, 26.3, 25.3, 20.6; HRESIMS *m*/*z*: $[M+Na]^+$. Calcd. for $C_{21}H_{31}NO_9Na$, 464.1997; Found 464.1997.

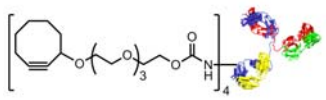

PEGO-IgG (13). A solution of carbonate **12** (20.8 µL, 65 µmol, 2.5 mg/mL in DMSO) was added to a solution of Anti-BSA Rabbit IgG (1.0 mL; 1.0 mg/mL in 10 mM PBS pH 7.4, 150 mM NaCl). After 1 h of moderate stirring at 25 ºC in the dark, the excess of unreacted **12** was removed by centrifugal ultrafiltration (Amicon® Ultra-4 centrifugal filters 50K, 5x3.5 mL; 10 mM PBS pH 7.4, 150 mM NaCl), affording pure **13**.

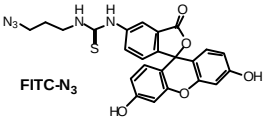

With the aim of determining the extent of antibody functionalization, **13** was treated with an excess of 1-(3-azidopropyl)-3-(3',6'-dihydroxy-3-oxo-3H-spiro[isobenzofuran-1,9'-xanthene]-5-yl)thiourea (FITC-N_3),[29] and the Fluorescein:IgG ratio calculated by UV-Vis according to the method of The, T. H. and Feltkamp, T. E.

W.[30] Briefly, a solution of FITC-N_3 in DMSO (50 µL, 0.388 mmol, 3.8 mg/mL) was added to a solution of **13** (1.0 mL; 0.3 mg/mL in 10 mM PBS pH 7.4, 150 mM NaCl). The reaction was shaken overnight at 25 ºC in the dark. Then, unreacted FITC-N_3 was removed by ultrafiltration (Amicon® Ultra-4 centrifugal filters 50K; 10 mM PBS pH 7.4, 150 mM NaCl) till no dye was detected in the filtrate by UV-Vis. A fluorescein/protein ratio (F/P) 4.1/1 was calculated according to the absorbance intensities at 280 and 495 nm.[30]

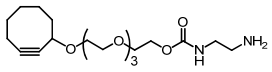

PEGO-NH_2 (14). Ethylenediamine (0.171 mL, 3.18 mmol, 2000 mol%) was added to a solution of carbonate **12** (70 mg, 0.159 mmol) in CH_2Cl_2 (1.6 mL). Reaction was allowed to stir at rt for 2 h, and then was concentrated under vacuum. The resulting crude product was purified by column chromatography (CH_2Cl_2/MeOH 15%) to give **14** (55 mg, 89%) as a colorless oil: ^{1}H NMR (250 MHz, $CDCl_3$, 300 K) δ: 6.25-6.08 (m, 1H), 4.31-4.00 (m, 5H), 3.79-3.40 (m, 14H), 3.36-3.22 (m, 2H), 2.90 (t, *J*=5.6 Hz, 2H), 2.30-1.24 (m, 10H); ^{13}C NMR (62 MHz, $CDCl_3$, 300K) δ: 156.6, 100.0, 92.5, 72.6, 70.3, 69.5, 68.2, 63.7, 42.1, 41.8, 40.9, 34.2, 29.6, 26.2, 20.5; HRESIMS *m*/*z*: $[M+H]^+$. Calcd. for $C_{19}H_{35}N_2O_6$, 397.2495; Found 397.2495.

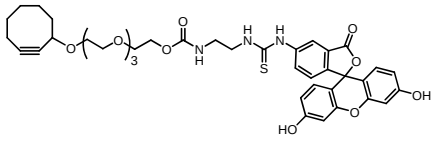

PEGO-FITC (15). A solution of **14** (50 mg, 0.129 mmol, 110 mol%), FITC (46 mg, 0.117 mmol), and DIPEA (0.136 mL, 0.781 mmol, 600 mol%) in DMF (1.19 mL) was stirred at rt for 16 h in the dark. After evaporation, the resulting crude product was dissolved in MeOH and precipitated by dropwise addition to a solution of 0.1 M HCl. The precipitate was filtered, washed with 0.1 M HCl and H_2O, and then dried under vacuum to give pure **15** (68 mg, 75%) as an orange solid: ^{1}H NMR (400 MHz, *d*-

DMSO, 353 K) δ: 9.79 (br s, 2H), 9.74 (br s, 1H), 8.23 (d, *J*=1.6 Hz, 1H), 7.90 (t, *J*=5.3 Hz, 1H), 7.79 (dd, *J*=1.6 Hz, *J*=8.2 Hz, 1H), 7.14 (d, *J*=8.2 Hz, 1H), 6.97 (br s 1H), 6.68 (d, *J*=2.1 Hz, 2H), 6.61 (d, *J*=8.7 Hz, 2H), 6.57 (dd, *J*=2.2 Hz, *J*=8.6 Hz, 2H), 4.24-4.18 (m, 1H), 4.09 (t, *J*=5.9 Hz, 2H), 3.69-3.39 (m, 16H), 3.27 (q, *J*=5.9 Hz, 2H), 2.28-1.33 (m, 10H); ^{13}C NMR (100 MHz, *d*-DMSO, 300K) δ: 180.6, 168.4, 159.4, 156.3, 151.7, 147.2, 141.1, 129.6, 128.9, 126.5, 124.0, 116.7, 112.4, 109.6, 102.1, 99.6, 93.1, 82.9, 71.7, 69.7, 69.5, 68.7, 63.2, 43.6, 41.8, 38.9, 33.7, 29.2, 25.8, 19.9; HRESIMS *m*/*z*: $[M+H]^+$. Calcd. for $C_{40}H_{46}N_3O_{11}S$, 776.2856; Found 776.2873.

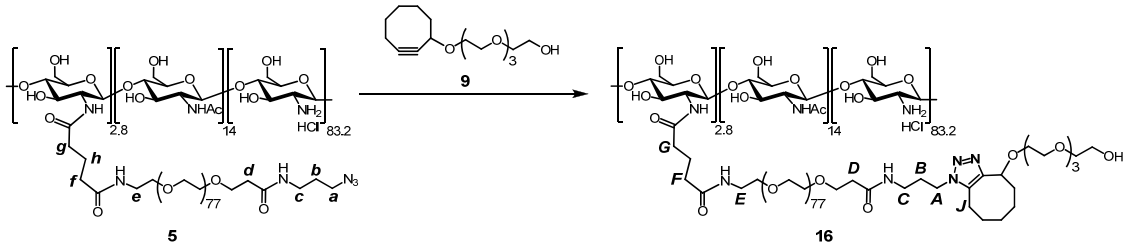

CS-*g*-PEG-OH (16): Monitoring of the Kinetics of the Strain-Promoted Click Functionalization of 5 as a Function of the Temperature. Three solutions of CS-*g*-PEG-N_3 **5** (15 mg, 50 μmol, DS 2.8) and PEGO-OH **9** (1.0 mg, 3.5 μmol, 7 mol%) in 85% H_2O/10% D_2O/5% *d*-DMSO (2.5 mL) were stirred at 25 º, 55 º and 80 ºC. The progress of the reactions was followed by presat ^{1}H NMR of aliquots (0.5 mL) taken at different times (acquisition time 1 s, delay time 0.1 s, saturation time 9 s, saturation power 2 dB). Complete functionalization was observed in all cases: 25 ºC (86 h, Figure S5), 55 ºC (13 h, Figure S6), and 80 ºC (4 h, Figure S7). In the spectra shown below, signals of **5** are in lowercase, while those of **16** in uppercase.

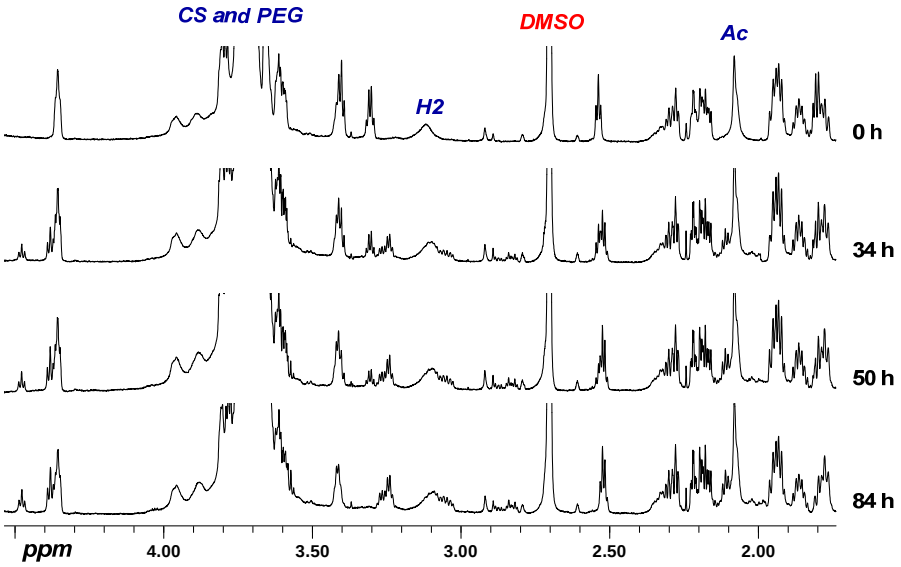

Figure S5. Monitoring the kinetics of the strain-promoted functionalization at 25 ºC by presat ^{1}H NMR (6 mg/mL, 85% H_2O/10% D_2O/5% *d*-DMSO, 750 MHz, 25 ºC).

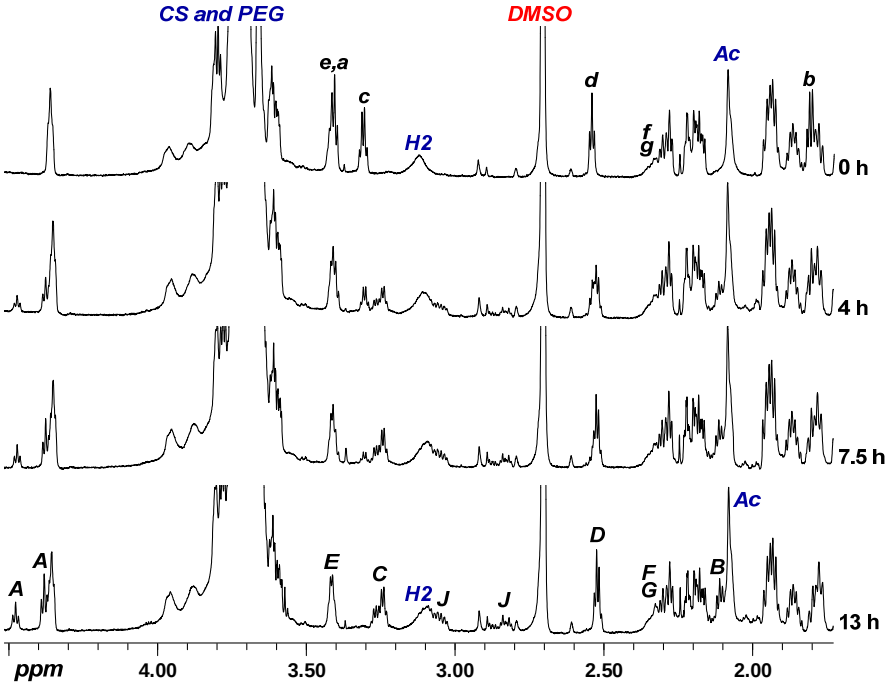

Figure S6. Monitoring the kinetics of the strain-promoted functionalization at 55 ºC by presat 1H NMR (6 mg/mL, 85% H_2O/10% D_2O/5% *d*-DMSO, 750 MHz, 25 ºC).

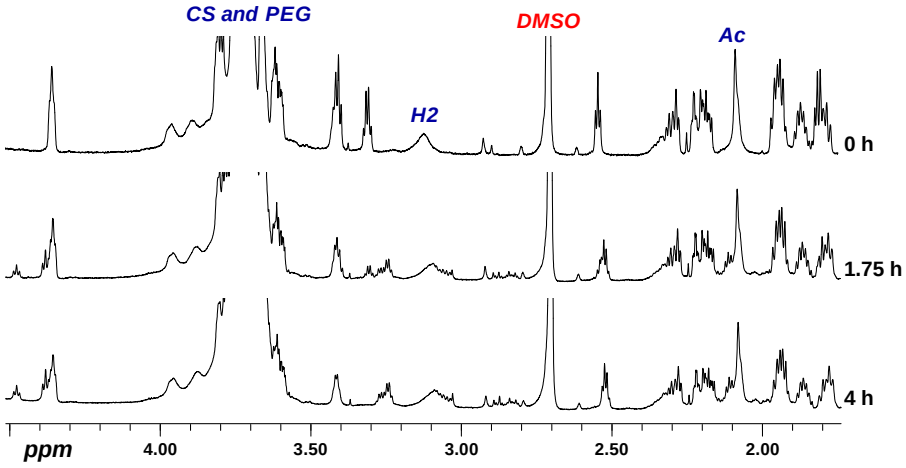

Figure S7. Monitoring the kinetics of the strain-promoted functionalization at 80 ºC by presat ^{1}H NMR (6 mg/mL, 85% H_2O/10% D_2O/5% *d*-DMSO, 750 MHz, 25 ºC).

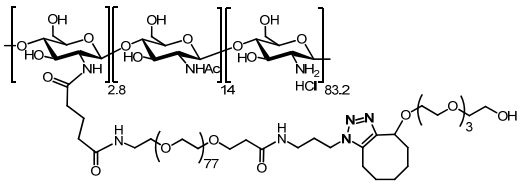

CS-*g*-PEG-OH (16): Preparation. Same reactions as above in 5% DMSO/H_2O (2.5 mL) were stirred for 86 h (25 ºC), 13 h (55 ºC), and 4 h (80 ºC) and then were ultrafiltered (Amicon® YM30, 10^{-3} M HCl and H_2O) and lyophilized to afford completely functionalized **16** (14-15 mg, 92-96% mass recovery) as a white foam: ^{1}H NMR (750 MHz, D_2O, 300 K) δ: 4.95 (m), 4.70-4.54 (m), 4.51-3.37 (m), 3.30-2.76 (m), 2.55-2.44 (m), 2.42-2.27 (m), 2.24-1.82 (m), 1.82-1.07 (m).

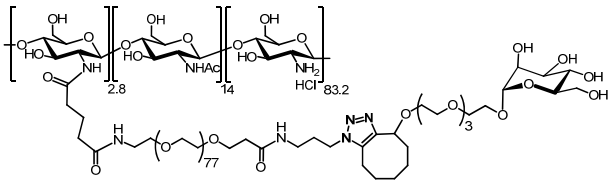

CS-*g*-PEG-Man (17). A solution of CS-*g*-PEG-N_3 **5** (15 mg, 50 µmol, DS 2.8) and PEGO-Man **11** (1.6 mg, 3.5 µmol, 7 mol%) in 5% DMSO/H_2O (2.5 mL) was stirred at 55 ºC for 24 h. Then, reaction

was ultrafiltered (Amicon® YM30, 10^{-3} M HCl and H_2O), and lyophilized to afford completely functionalized **17** (15 mg, 95% mass recovery) as a white foam: ^{1}H NMR (750 MHz, D_2O, 300 K) δ: 4.95 (m), 4.70-4.54 (m), 4.51-3.37 (m), 3.30-2.76 (m), 2.55-2.44 (m), 2.42-2.27 (m), 2.24-1.82 (m), 1.82-1.12 (m).

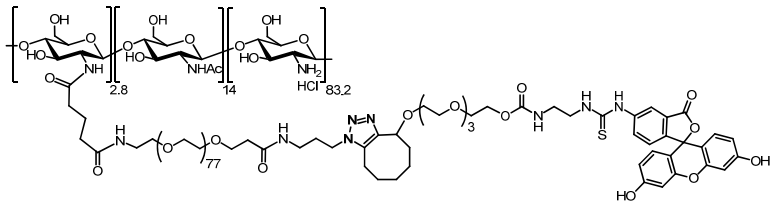

CS-*g*-PEG-FITC (18). A solution of CS-*g*-PEG-N_3 **5** (15 mg, 50 μmol, DS 2.8) and PEGO-FITC **15** (2.7 mg, 3.5 μmol, 7 mol%) in 25% DMSO/H_2O (2.5 mL, pH 6.7) was stirred at 55 ºC for 40 h. Then, reaction was ultrafiltered (Amicon® YM30, 10^{-3} M HCl and H_2O) and lyophilized to afford completely functionalized **18** (15 mg, 96% mass recovery) as an orange foam: ^{1}H NMR (750 MHz, D_2O, 300 K) δ: 8.54-8.44 (m), 7.96-7.62 (m), 7.40-7.29 (m), 6.85-6.66 (m), 4.95 (m), 4.70-4.54 (m), 4.46-3.29 (m), 3.28-2.68 (m), 2.55-2.44 (m), 2.42-2.27 (m), 2.24-1.82 (m), 1.75-1.01 (m).

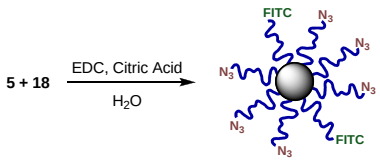

Preparation of Clickable CS-*g*-PEG-N_3 Fluorescent Nanoparticles (19). The pH of a solution of citric acid in H_2O (8.9 mg/mL) was adjusted to 6.5 with NaOH. Then, EDC·HCl was added up to a concentration of 15.6 mg/mL while stirring at 0 ºC. After 30 min, an aliquot of this activated citric acid solution was added to a solution of CS-*g*-PEG-N_3 **5** (0.97 mg/mL, DS 0.5) and CS-*g*-PEG-FITC **18** (0.03 mg/mL, DS 2.8) in H_2O at pH 5.7 (15 μL of citric acid-EDC·HCl solution per 1 mL CS-*g*-PEG solution). Reaction was allowed to moderately shake at rt for 2 h. The resulting solution of CS-*g*-PEG-

N_3 fluorescent NP **19** was purified by dialysis against MilliQ water overnight at 4 ºC. NP **19** were characterized by DLS, TEM and AFM.

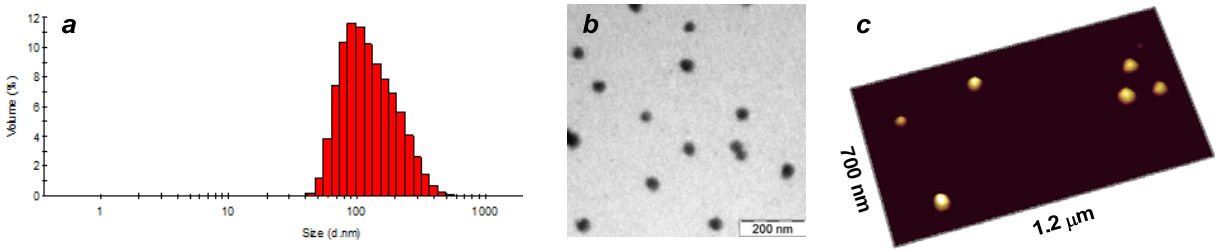

Figure S8. DLS histogram of NP **19** in H_2O at 25 ºC (***a***). TEM (***b***) and tapping mode AFM (***c***) images of NP **19** in H_2O.

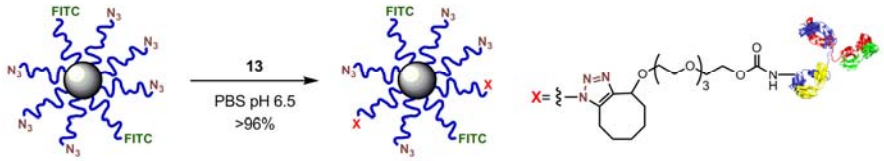

Clicking PEGO-IgG (13) to CS-*g*-PEG-N_3 Fluorescent Nanoparticles (19). Preparation of Immuno-Nanoparticles (20). A solution of NP **19** (0.9 mL, 1.0 mg/mL) was diluted with 100 mM PBS pH 6.5, 1.5 M NaCl (0.1 mL). Then, a solution of PEGO-IgG **13** (9 µL, 1.0 mg/mL in 10 mM PBS pH 7.4, 150 mM NaCl, 0.3 mol% per N_3) was added (**13**:**19** mass ratio 1:100). The resulting solution was stirred at 25 ºC for 7 h in the dark to furnish IgG functionalized immuno-NP **20**.

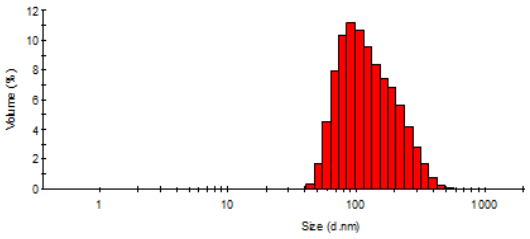

Figure S9. DLS histogram of immuno-NP **20** in H_2O at 25 ºC.

Quantification of PEGO-IgG (13) incorporated to Immuno-Nanoparticles (20) by Dot Blot. Glucose was added (4% w/v) to a solution of clickable NP **19**. After NP isolation by ultracentrifugation on a glucose bed (30000 g x 30 min, 10 ºC), they were resuspended in 10 mM PBS pH 6.5, 150 mM NaCl and were incubated with PEGO-IgG **13** (cyclooctyne Anti-BSA Rabbit IgG conjugate) at 25 ºC for 7 h (**19**:**13** mass ratio, 100:1). The resulting immuno-NP **20** were ultracentrifuged again (60000 g x 20 min, 10 ºC) and the supernatant was analyzed by Dot Blot to determine the amount of unreacted **13**. Briefly, an aliquot of the supernatant (5 µL) was spotted on a PVDF membrane. The membrane was blocked by soaking in a solution of powder milk (45 min, rt), then it was washed with TNT buffer and incubated with a 1:10000 solution of HRP conjugated Goat Anti-Rabbit IgG at rt for 1 h. After washing again, the membrane was incubated with a 1:1 mixture of Luminol/Enhancer Solution® and Stable Peroxide Solution® for 5 min in the dark. Then, it was exposed to a CL-XPosure™ film. The photographic film was revealed, and the intensity of the signals was measured with a ChemDoc™ XRS densitometer using Quantity One software. The incorporation of PEGO-IgG **13** to the surface of immuno-NP **20** was determined to be higher than 96% by comparison with standards of PEGO-IgG **13** of known concentration.

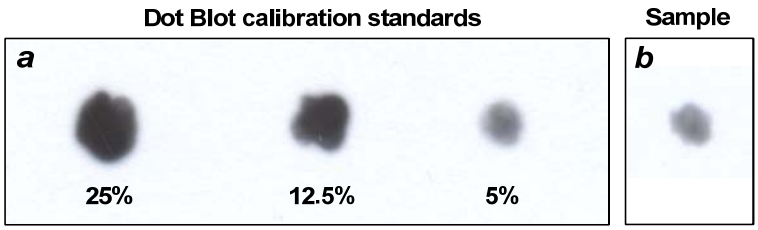

Figure S10. Determination by Dot Blot of unbound PEGO-IgG **13** to immuno-NP **20**. Calibration standards with concentrations 25%, 12.5% and 5% of initial **13** (***a***). Supernatant after 7 h of incubation at 25 ºC (***b***).

Average number of IgG per Immuno-Nanoparticle (20). With the aim of calculating the number of IgG per immuno-NP **20**, NP **19** were considered as hard spheres with a diameter of 47 nm (TEM). From the volume calculated for a single NP, and taken into account the densities of CS (1.42 g/mL)[31] and PEG (1.12 g/mL),[32] a MW of $4.6 \cdot 10^7$ was estimated for NP **19**. From these data and by considering the M_w of CS-*g*-PEG-N_3 (DS 0.5, $8.7 \cdot 10^4$) and CS-*g*-PEG-FITC (DS 2.8, $1.3 \cdot 10^5$), an average of 1025 PEG-N_3 and 115 PEG-FITC chains result per NP **19**. According to Dot Blot analyses, as >96% of the initial PEGO-IgG **13** was effectively conjugated to NP **19**, an average of 3.0 IgG per immuno-NP **20** was estimated.

Incubation of BSA-Agarose Beads with Anti-BSA IgG Functionalized Fluorescent Immuno-Nanoparticle (20). A suspension of BSA-Agarose beads (25 µL, 10.1 mg/mL in 10 mM PBS pH 7.4, 150 mM NaCl) was added to a solution of Anti-BSA IgG functionalized fluorescent immuno-NP **20** (1.0 mL, 1.0 mg/mL in 10 mM PBS pH 6.5, 150 mM NaCl). The resulting suspension was shaken in the dark for 2 h at 37 ºC. Then, the beads were centrifuged (1000 g, 30 s), washed (10 mM PBS pH 6.5, 150 mM NaCl) and centrifuged again. After three additional washing/centrifugation cycles, beads were finally suspended in 10 mM PBS pH 7.4, 150 mM NaCl and analyzed by laser scanning confocal microscopy (LSCM) on a Leica TCS SP2 Laser Scanning Spectral Confocal Microscope equipped with HC PL APO CS20X/0.7 dry objective lens. Excitation of fluorescent BSA-Agarose beads was carried out with an Ar laser at 488 nm, and emission was collected between 492-550 nm. BSA-Agarose beads treated with unfunctionalized fluorescent NP **19** under identical conditions served as control.

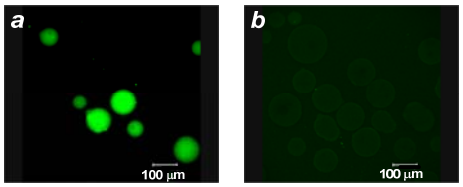

Figure S11. LSCM images of BSA-Agarose beads stained by fluorescent immuno-NP **20** (***a***), and fluorescent NP **19** as control (***b***).

NMR Spectra of New Compounds

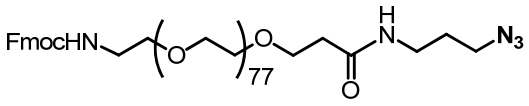

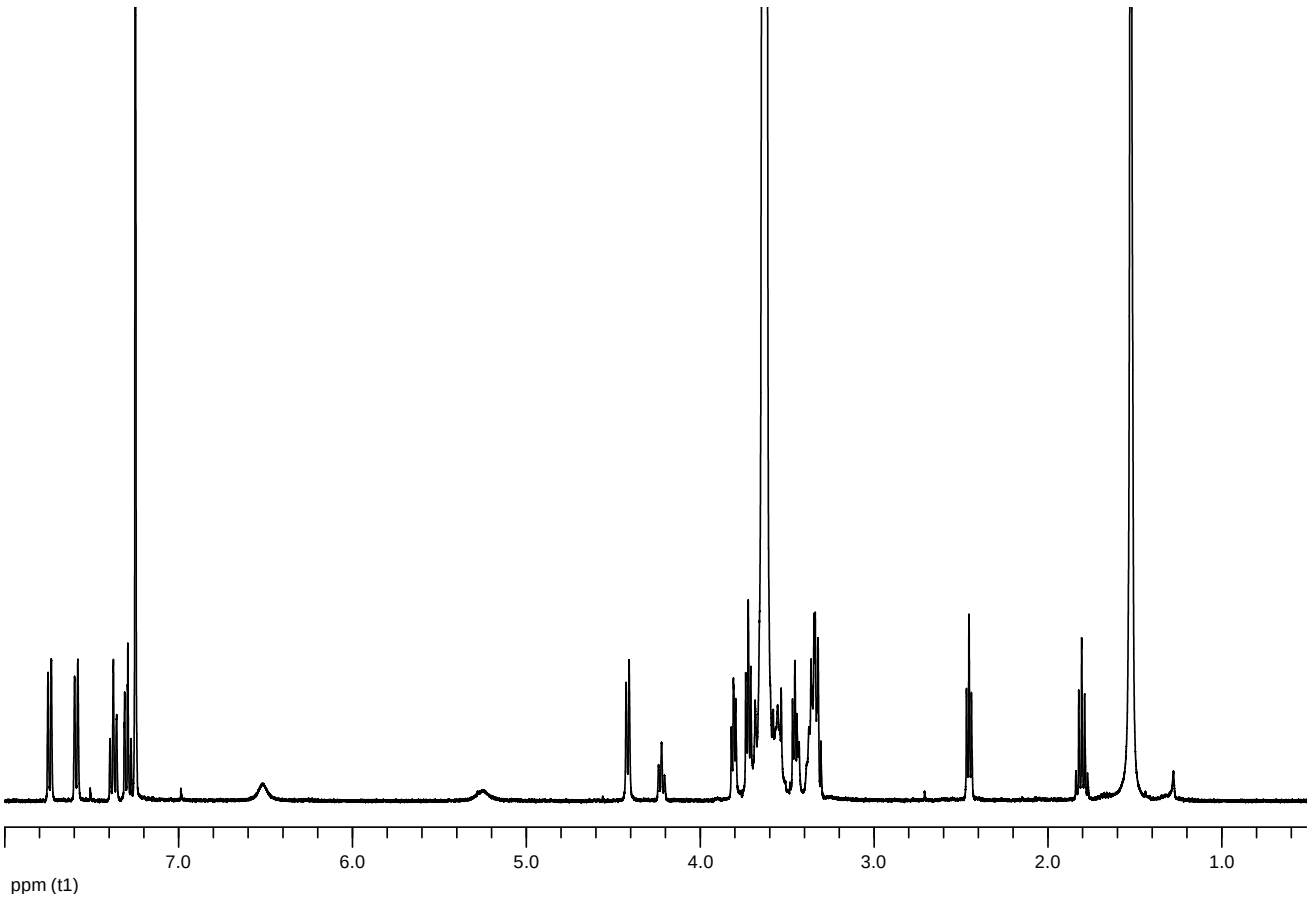

^{1}H NMR spectrum of N_3-PEG-NHFmoc **(2)** in $CDCl_3$.

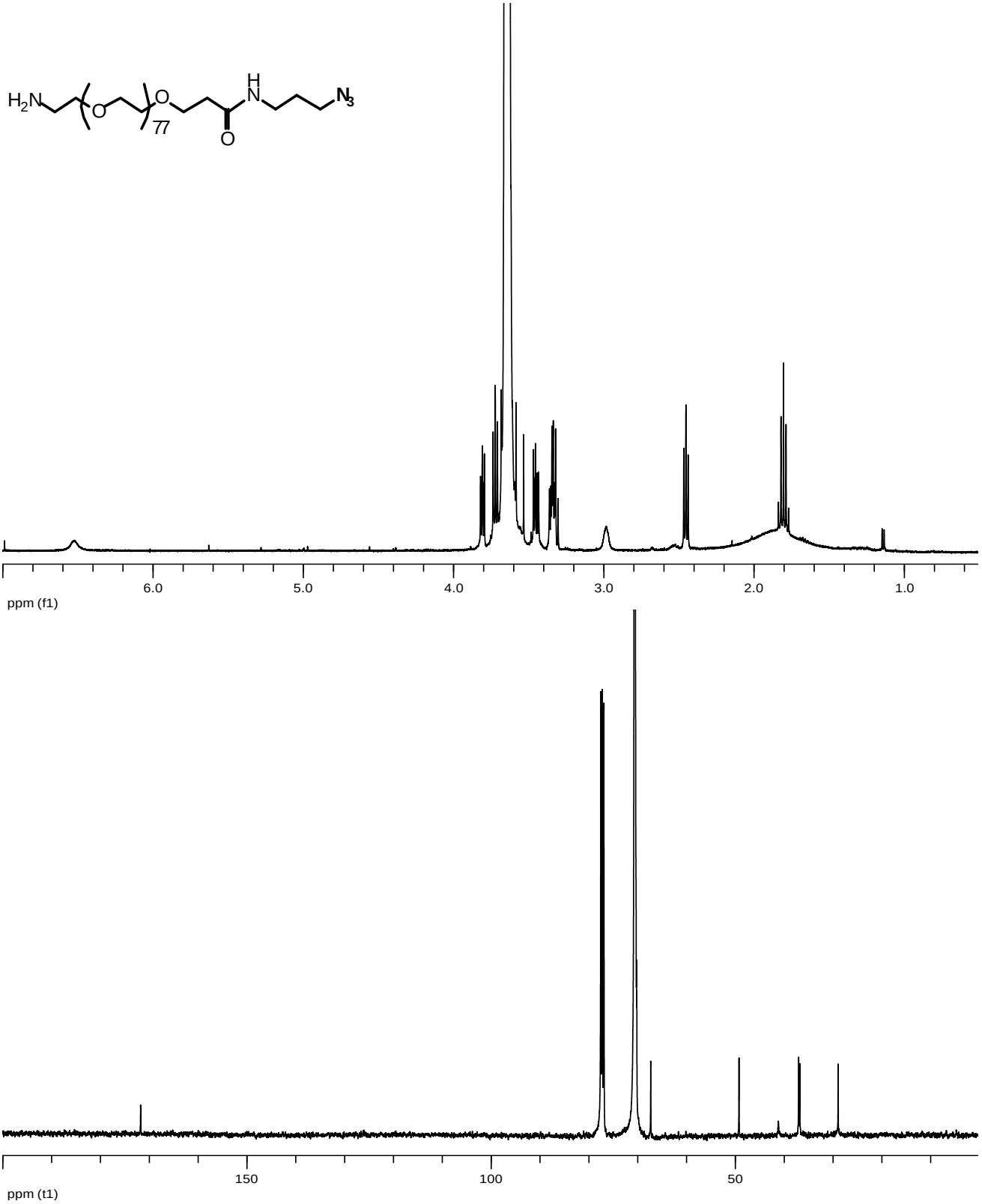

^{1}H NMR and ^{13}NMR spectra of N_3-PEG-NH_2 **(3)** in $CDCl_3$.

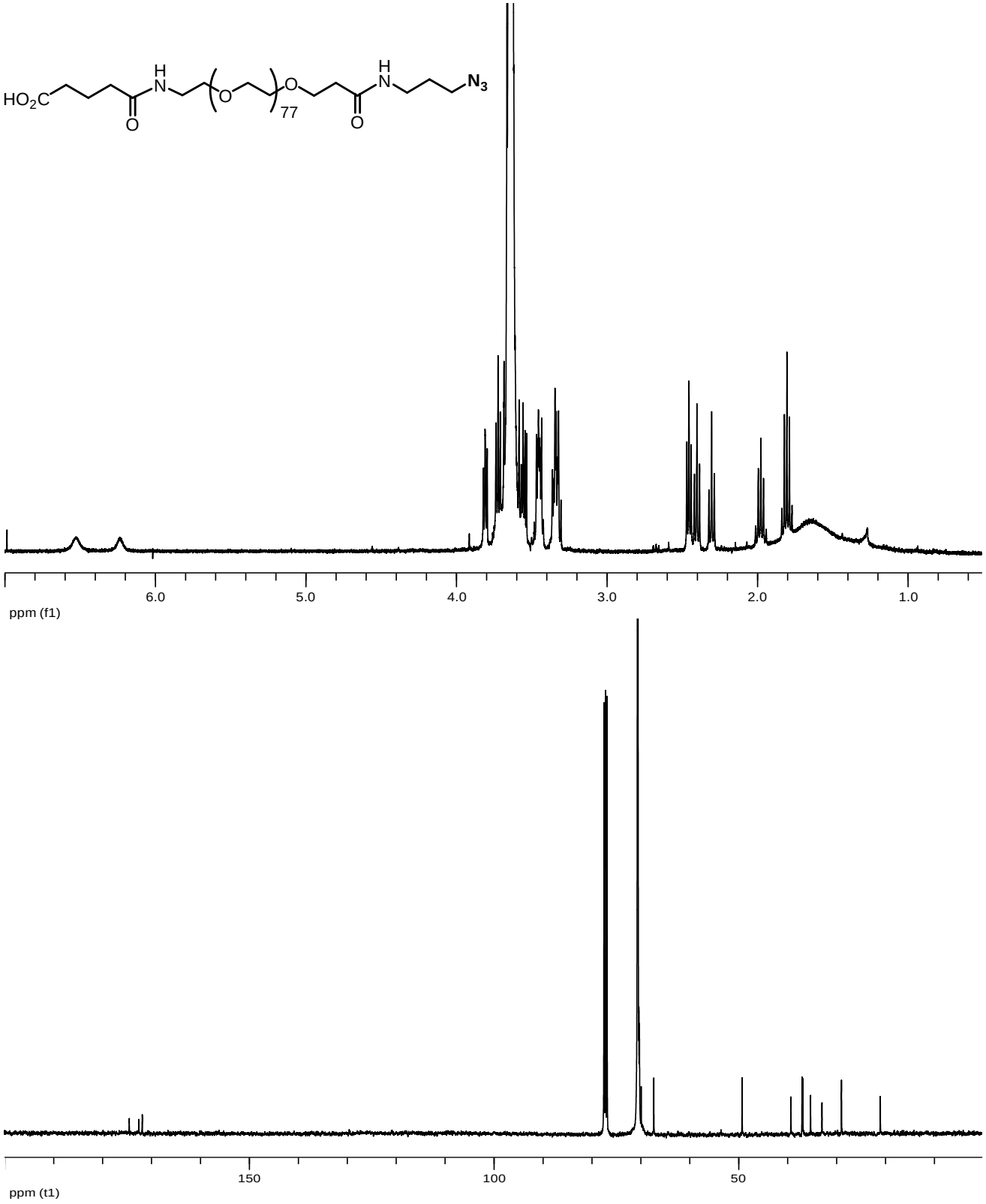

^{1}H NMR and ^{13}NMR spectra of N_3-PEG-CO_2H **(4)** in $CDCl_3$.

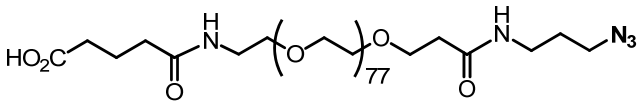

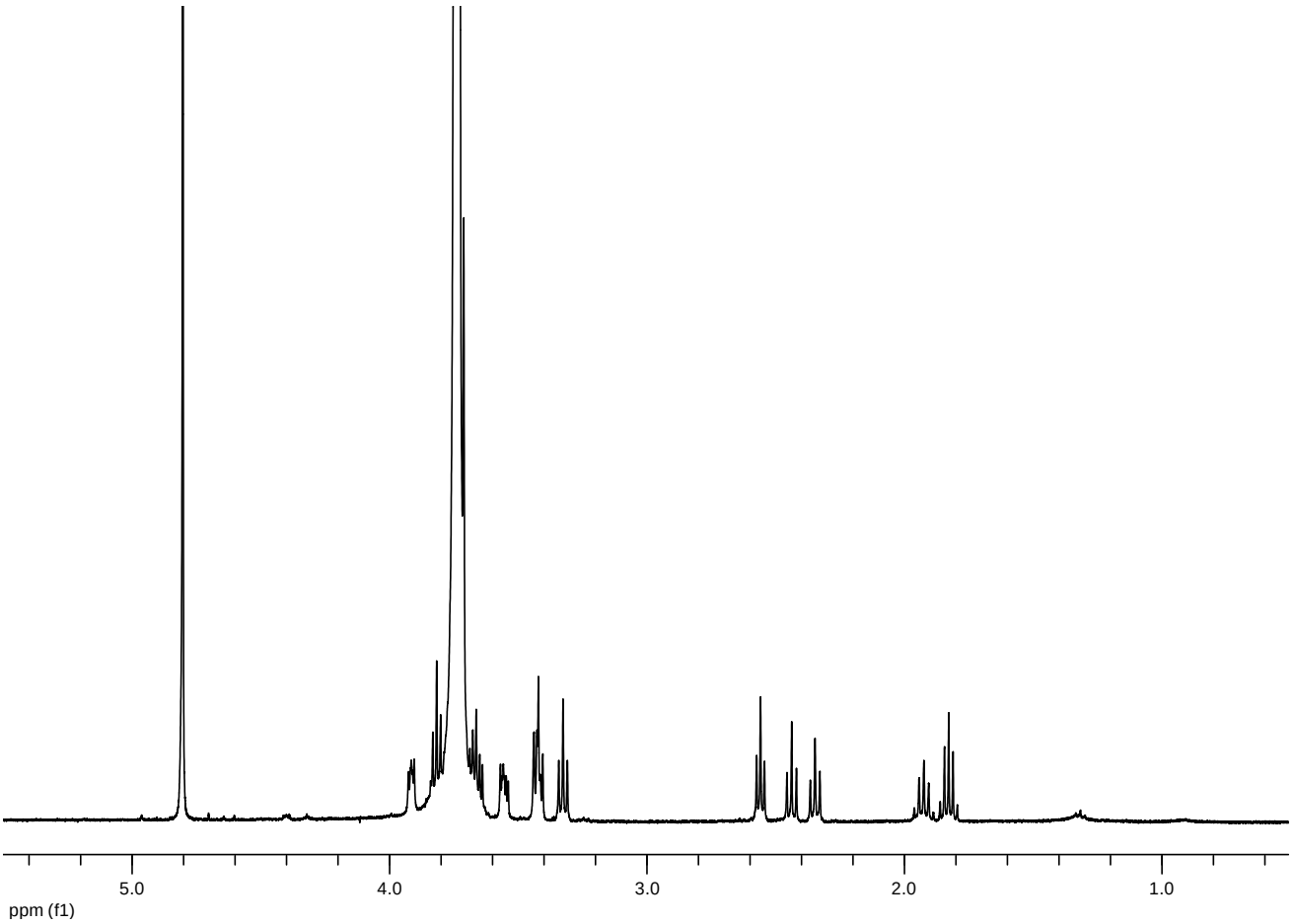

^{1}H NMR spectrum of N_3-PEG-CO_2H **(4)** in D_2O.

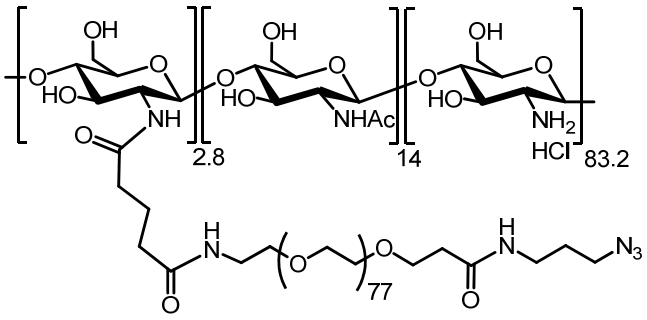

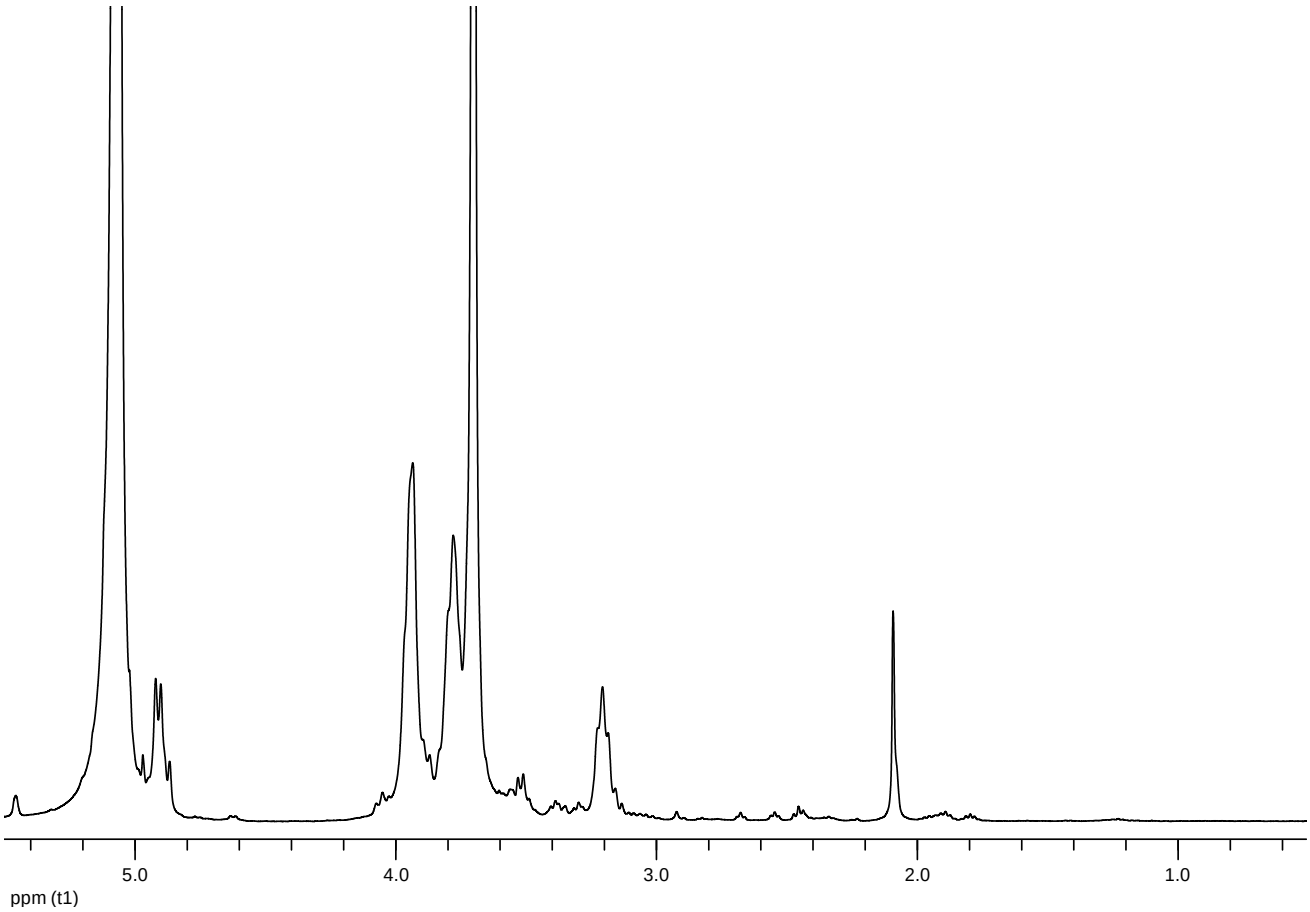

^{1}H NMR spectrum of CS-*g*-PEG-N_3 **(5)** (DS 2.8) in 2% DCl in D_2O.

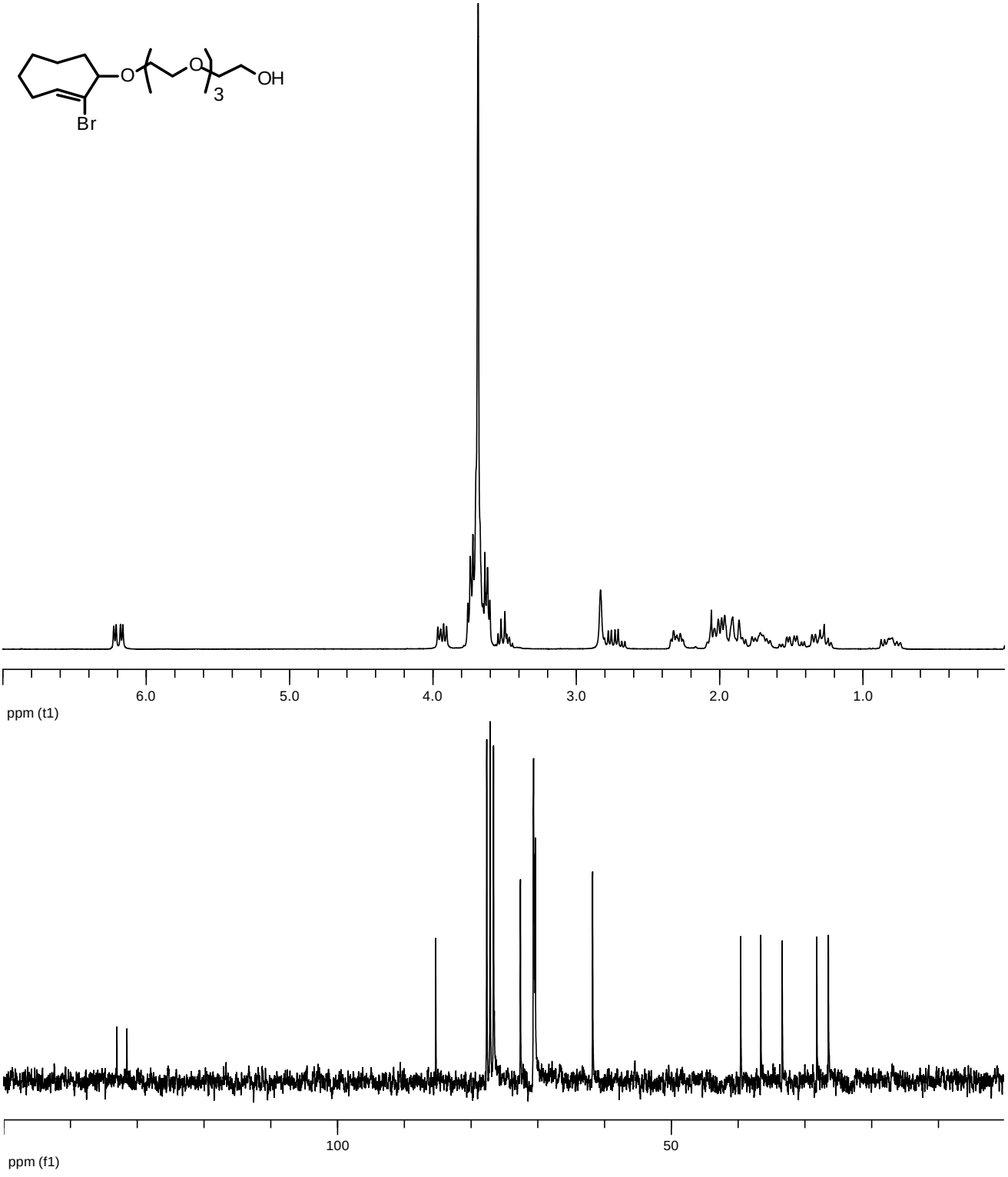

^{1}H NMR and ^{13}C NMR spectra of alcohol **(8)** in $CDCl_3$.

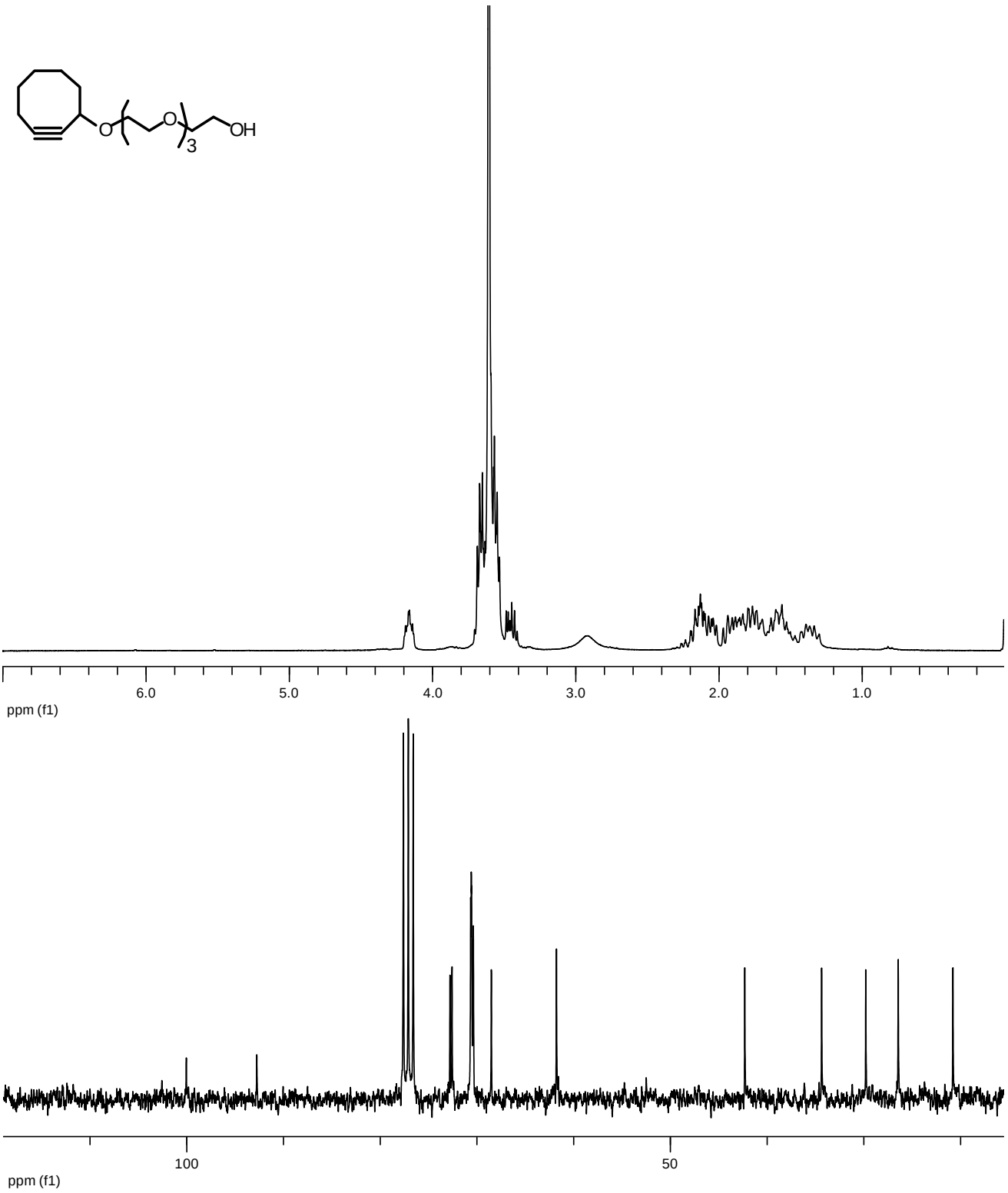

^{1}H NMR and ^{13}C NMR spectra of PEGO-OH **(9)** in $CDCl_3$.

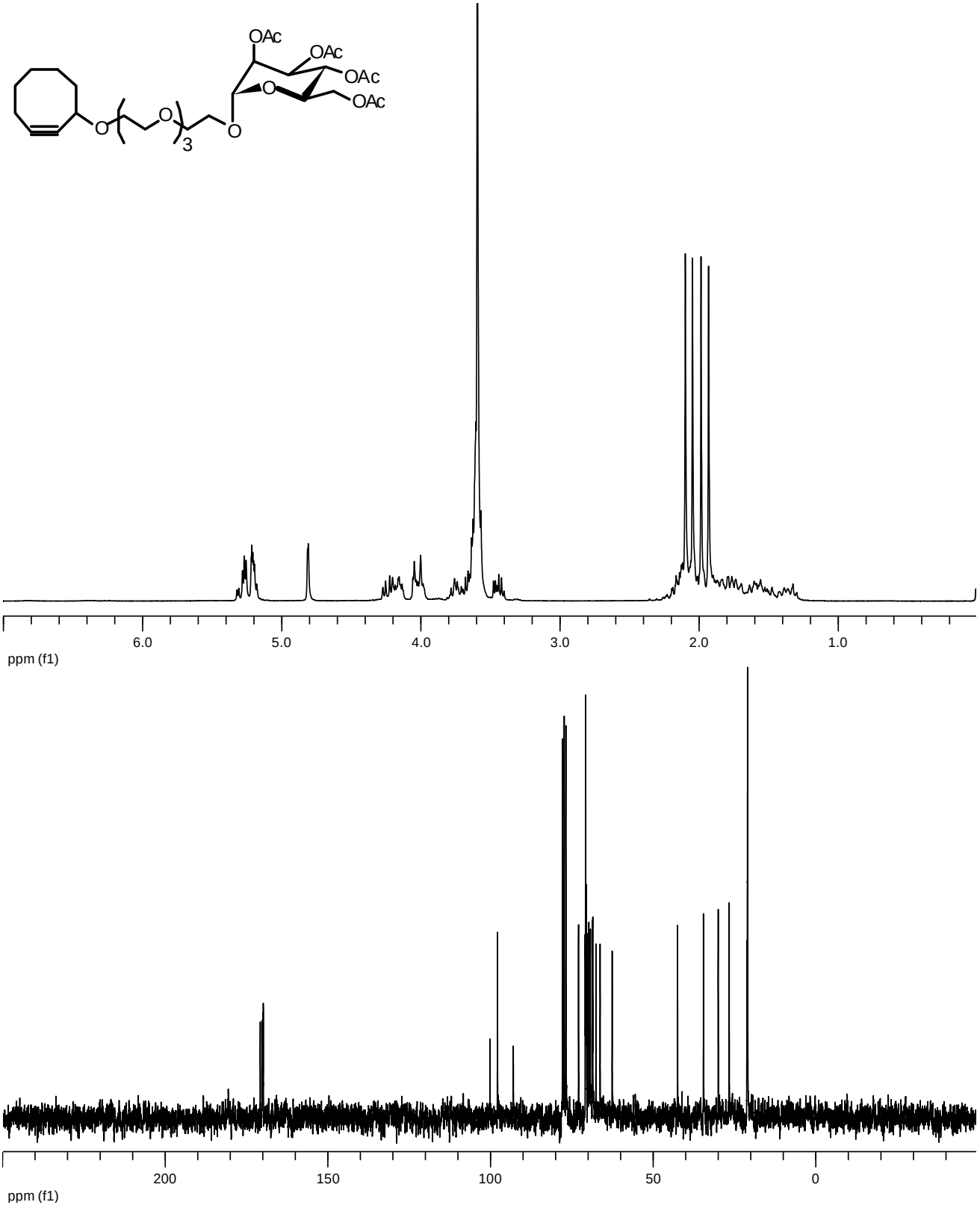

^{1}H NMR and ^{13}C NMR spectra of PEGO-Man-OAc **(10)** in $CDCl_3$.

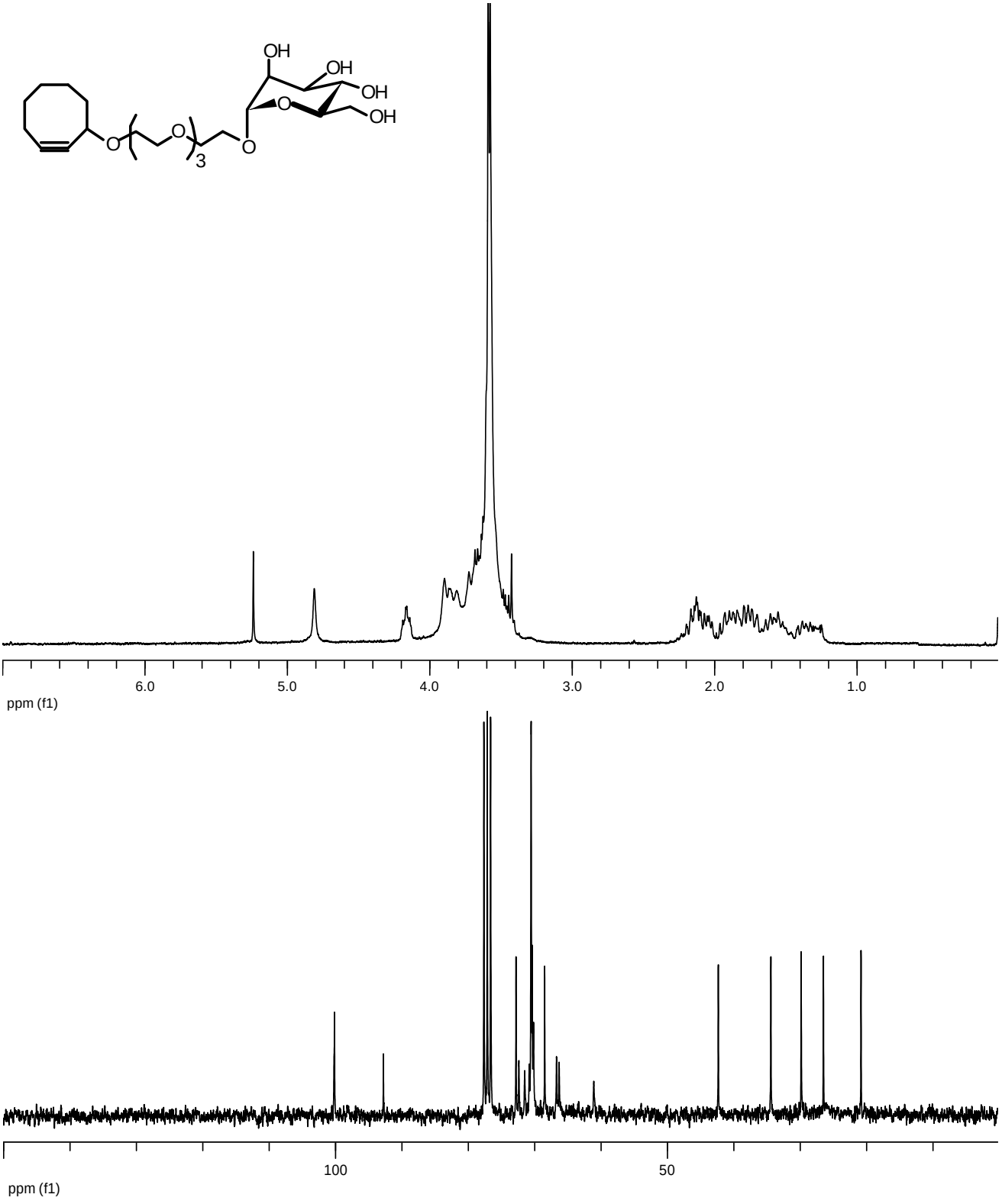

^{1}H NMR and ^{13}C NMR spectra of PEGO-Man **(11)** in $CDCl_3$.

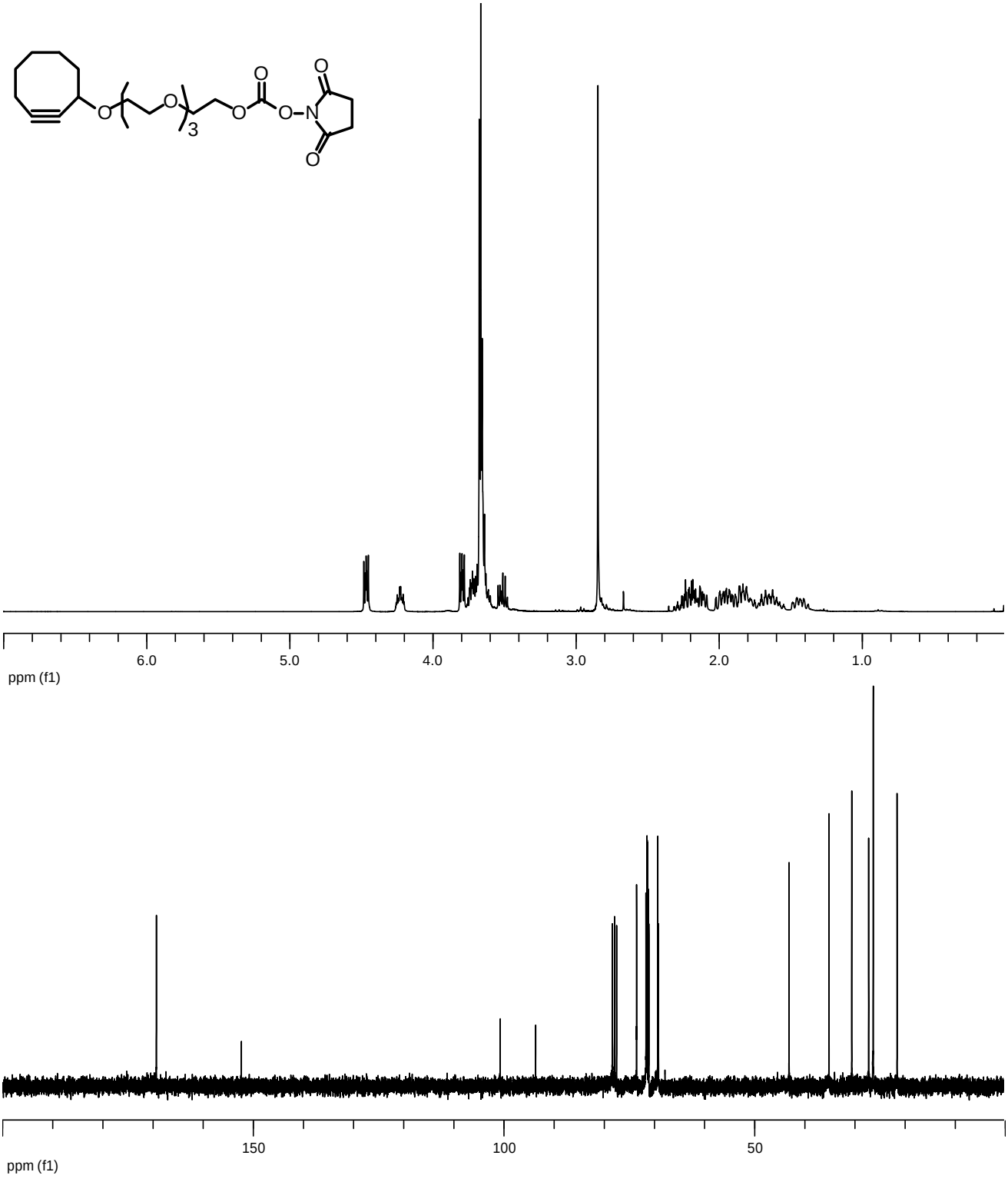

^{1}H NMR and ^{13}C NMR spectra of PEGO-NHS **(12)** in $CDCl_3$.

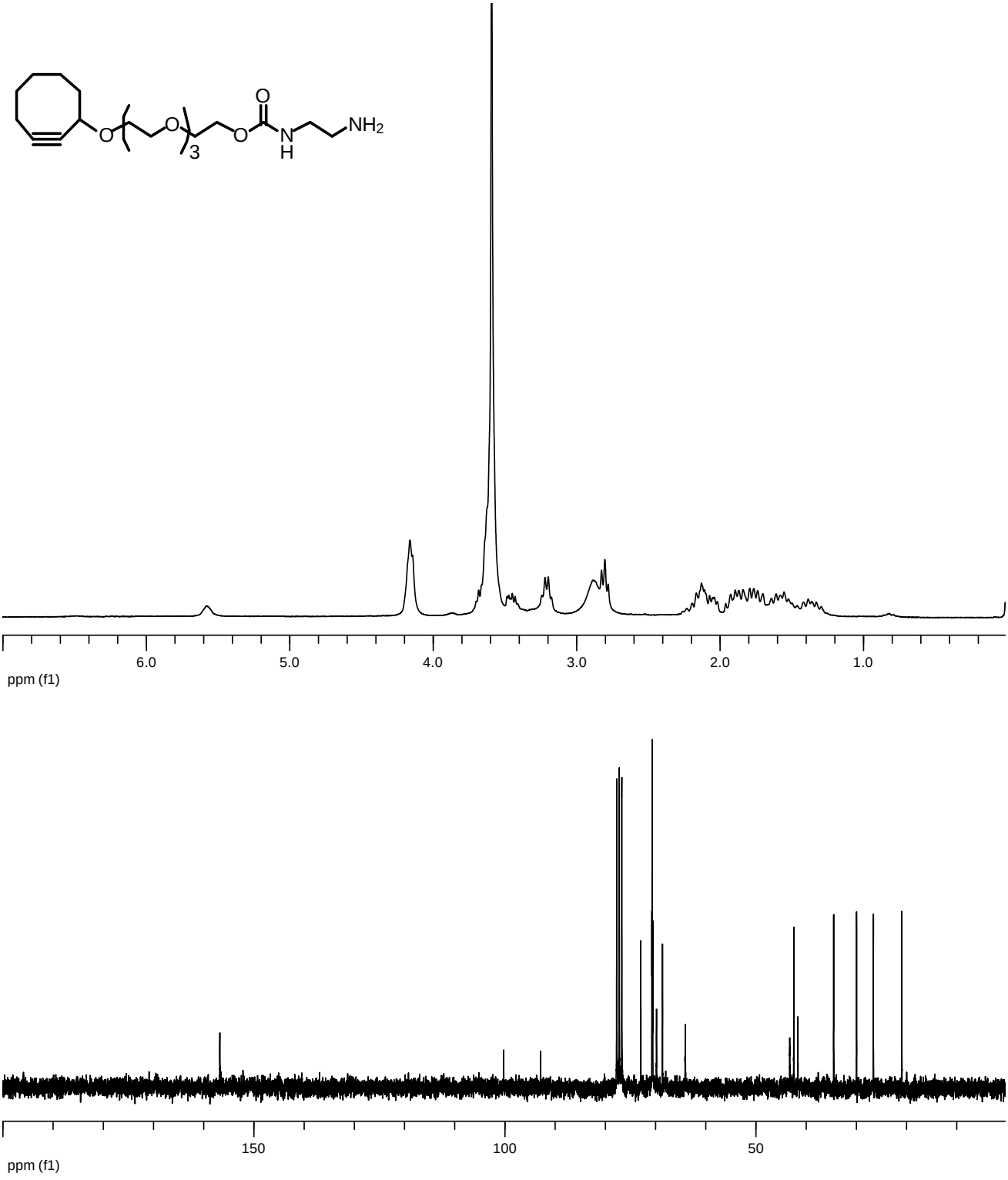

^{1}H NMR and ^{13}C NMR spectra of PEGO-NH_2 **(14)** in $CDCl_3$.

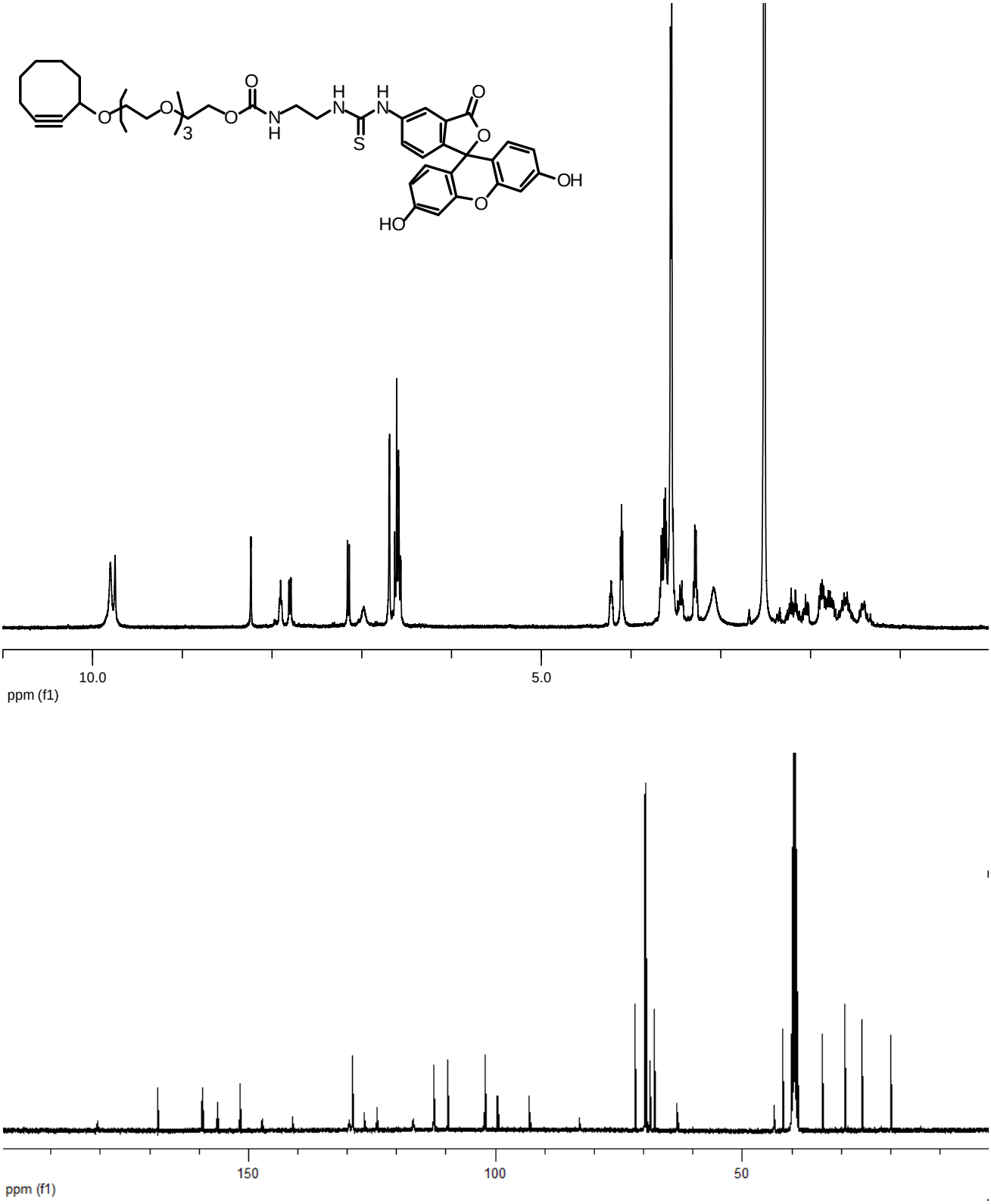

^{1}H NMR and ^{13}C NMR spectra of PEGO-FITC **(15)** in *d*-DMSO.

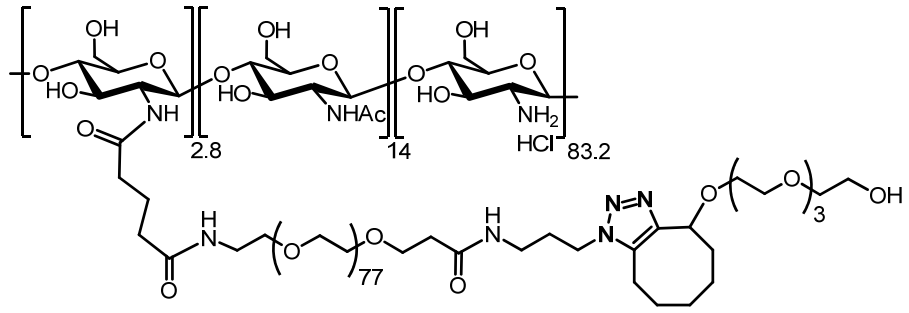

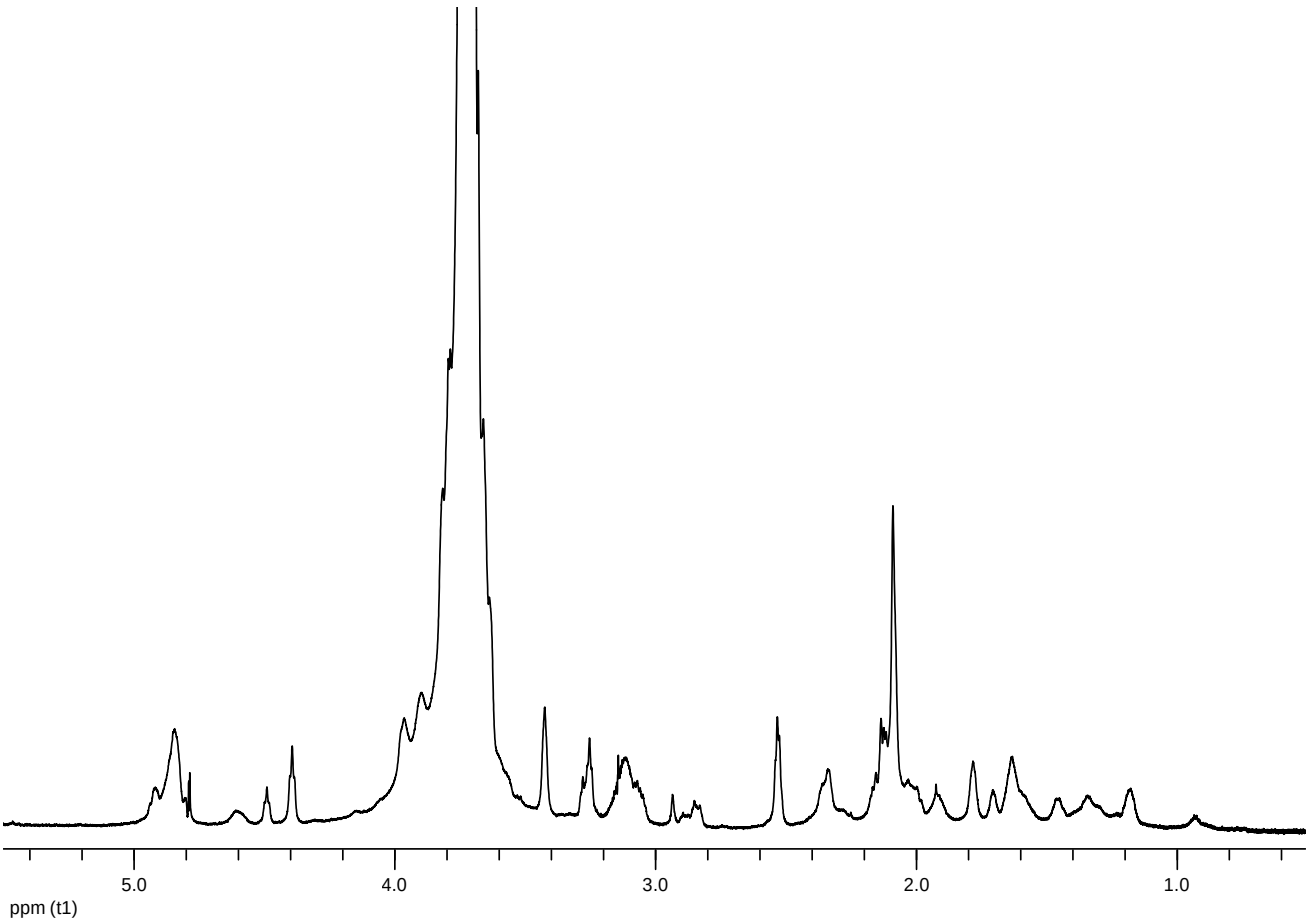

Presat ^{1}H NMR spectrum of CS-*g*-PEG-OH **(16)** in D_2O.

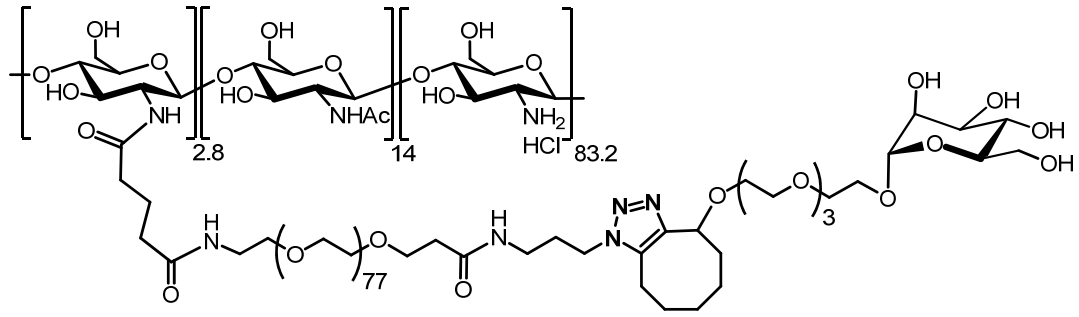

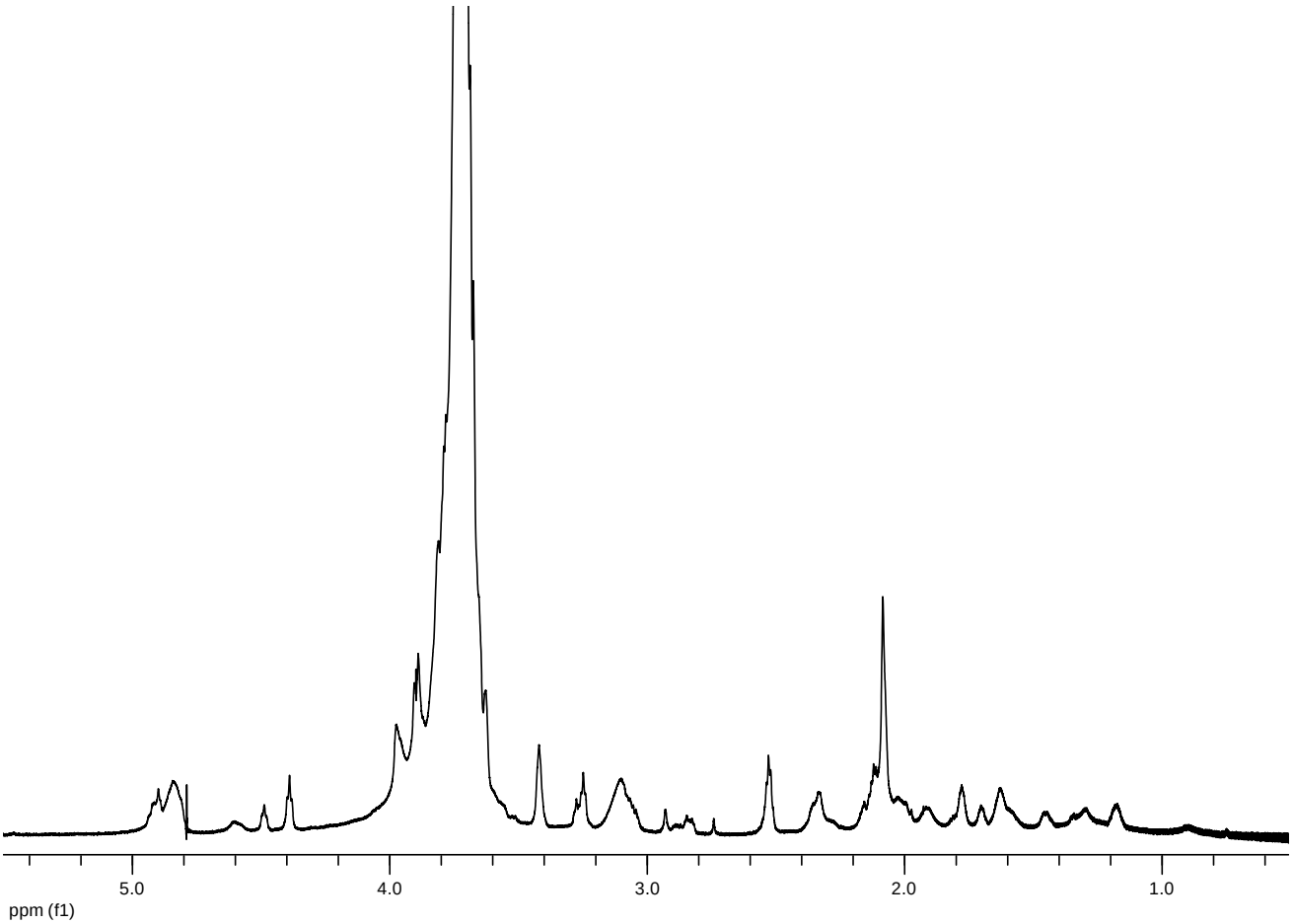

Presat ^{1}H NMR spectrum of CS-*g*-PEG-Man **(17)** in D_2O.

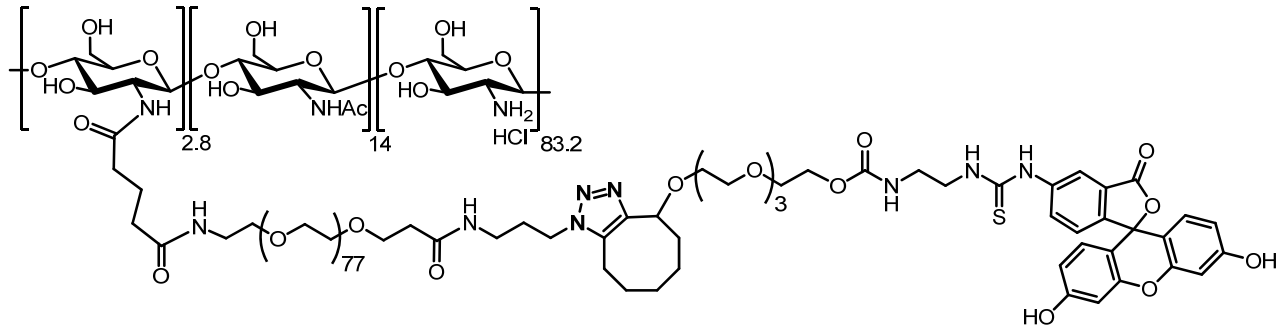

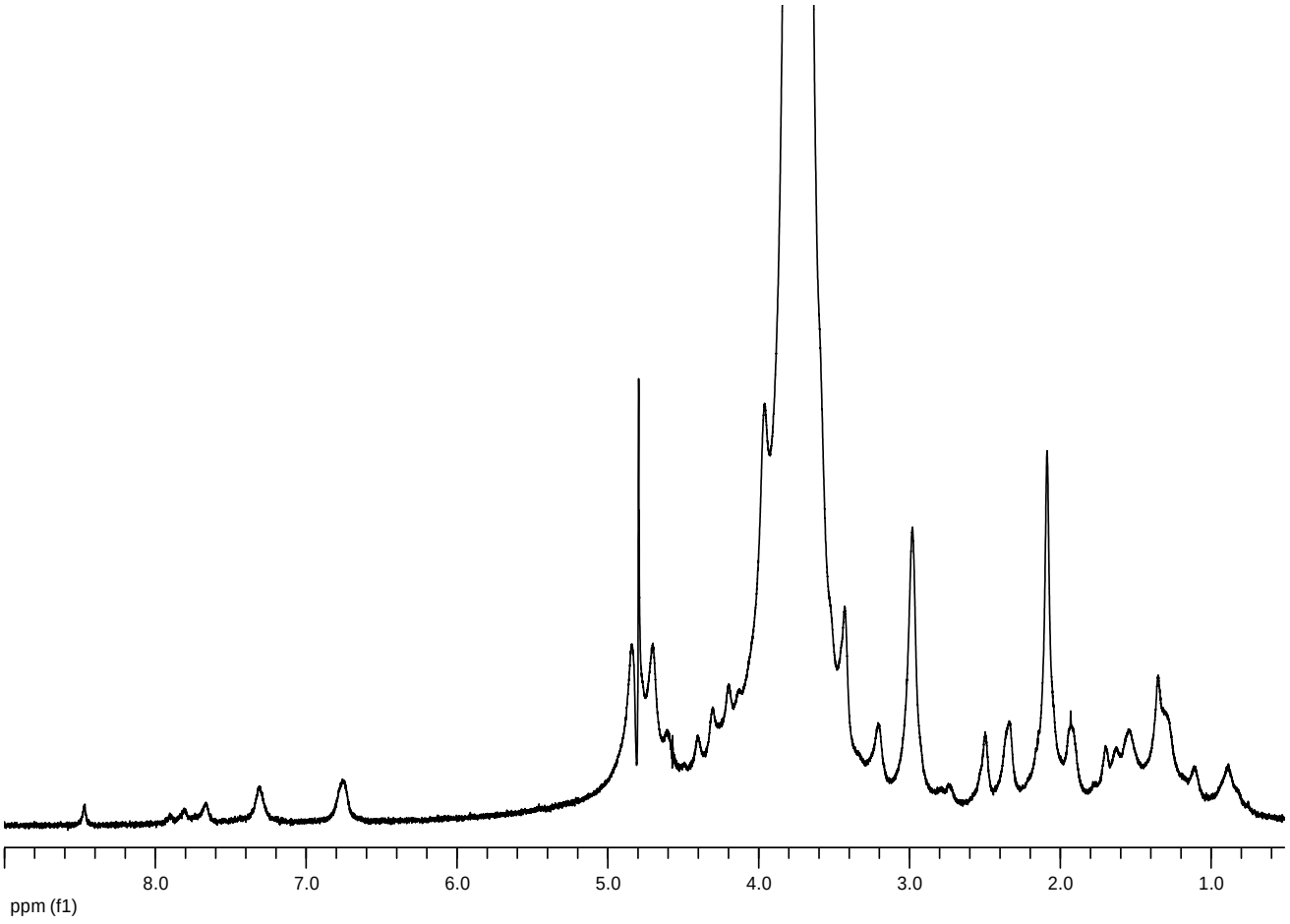

Presat ^{1}H NMR spectrum of CS-*g*-PEG-FITC **(18)** in D_2O.

1 Fernandez-Megia, E.; Novoa-Carballal, R.; Quiñoá, E.; Riguera, R. *Carbohydr. Polym.* **2005**, *61*, 155.

2 Kubas, G. J. *Inorg. Synth.* **1979**, *19*, 90.

3 (a) Lamarque, G.; Lucas, J. M.; Viton, C.; Domard, A. *Biomacromolecules* **2005**, *6*, 131. (b) Schatz, C.; Pichot, C.; Delair, T.; Viton, C.; Domard, A. *Langmuir* **2003**, *19*, 9896.

4 Cordeiro, L. C. M.; Reis, R. A.; Tischer, C. A.;. Gorin, F. A. J; Ferreira, J. C.; Iacomini, M. *FEMS Microbiol. Lett.* **2003**, *220*, 89.

5 American Polymer Standards Corporation: http://www.ampolymer.com/dndc.htm

6 Hokputsa, S.; Jumel, K.; Alesander, C.; Harding, S. E. *Carbohydr. Polym.* **2003**, *52*, 111.

7 Fry, S. C. *Biochem. J.* **1998**, *332*, 507.

8 Miller, A. R. *Biochem. Biophys. Res. Commun.* **1986**, *141*, 238.

9 Tabbì, G.; Fry, S. C.; Bonomo, R. P. *J. Inorg. Biochem.* **2001**, *84*, 179.

10 Bonomo, R. P.; Marchelli, R.; Tabbì, G. *J. Inorg. Biochem.* **1995**, *60*, 205.

11 Uchiyama, H.; Dobashi, Y.; Ohkouchi, K.; Nagasawa, K. *J. Biol. Chem.* **1990**, *265*, 7753. and referenced therein.

12 Hawkins, C. L.; Davies, M. J. *Free Radical Biol. Med.* **1996**, *21*, 275.

13 Soltés, L.; Mendichi, R.; Kogan, G.; Schiller, J.; Stankovská, M.; Arnhold, J. *Biomacromolecules* **2006**, *7*, 659.

14 Crescenzi, V.; Belardinelli, M.; Rinaldi, C. *J. Carbohydr. Chem.* **1997**, *16*, 561.

15 Wong, S. F.; Halliwell, B.; Richmond, R.; Skowroneck, W. R. *J. Inorg. Biochem.* **1981**, *14*, 127.

16 Uchida, K.; Kawakishi, S. *Agric. Biol. Chem.,* **1986**, *50*, 367.

17 Tanioka, S.; Matsui, Y.; Irie, T.; Tanigawa, T.; Tanaka, Y.; Shibata, H.; Sawa, Y.; Kono, Y. *Biosci., Biotechnol., Biochem.* **1996**, *60*, 2001.

18 Yin, X.; Zhang, X.; Lin, Q.; Feng, Y.; Yu, W.; Zhang, Q. *Arkivoc* **2004**, 66.

19 Nordtveit, R. J.; Varum, K. M.; Smidsrod, O. *Carbohydr. Polym.* **1994**, *23*, 253.

20 Chang, K. L. B.; Tai, M.-C.; Cheng, F.-H. *J. Agric. Food Chem.* **2001**, *49*, 4845.

21 Qin, C. Q.; Du, Y. M.; Xiao, L. *Polym. Degrad. Stabil.* **2002**, *76*, 211.

22 Zoldners, J.; Kiseleva, T.; Kaiminsh, I. *Carbohydr. Polym.* **2005**, *60*, 215.

23 Harish Prashanth, K. V.; Dharmesh, S. M.; Jagannatha Rao, K. S.; Tharanathan, R. N. *Carbohydr. Res.* **2007**, *342*, 190.

24 Ulanski, P.; von Sonntag, C. *J. Chem. Soc., Perkin Trans. 2* **2000**, 2022.

25 Tai, C.; Peng, J.-F.; Liu, J.-F.; Jiang, G.-B.; Zou, H. *Anal. Chim. Acta* **2004**, *527*, 73.

26 Carboni, B.; Benalil, A.; Vaultier, M. *J. Org. Chem.* **1993**, *58*, 3736.

27 Skattebol, L.; Solomon, S. *Organic Syntheses* **1973**, *5*/Coll. Volumes, 306.

28 (a) Ren, T.; Liu, D. *Tetrahedron Lett.* **1999**, *40*, 7621. (b) Nagahori, N.; Nishimura, S.-I. *Biomacromolecules* **2001**, *2*, 22.

29 Lin, P.-C.; Ueng, S.-H.; Tseng, M.-C.; Ko, J.-L.; Huang, K.-T.; Yu, S.-C.; Adak, A. K.; Chen, Y.-J.; Lin, C.-C. *Angew. Chem., Int. Ed.* **2006**, *45*, 4286.

30 The, T. H.; Feltkamp, T. E. W. *Immunology* **1970**, *18*, 865.

31 Lao, L. Tan, H.; Wang, Y.; Gao, Ch. *Colloids and Surfaces B: Biointerfaces* **2008**, *66*, 218.

32 Li, C. Y.; Birnkrant, M. J.; Natarajan, L. V.; Tondiglia, V. P.; Lloyd, P. F.; Sutherland, R. L.; Bunning, T. J. *Soft. Matter.* **2005**, *1*, 238.